UNIVERSITA' DEGLI STUDI DI MILANO

FACOLTA' DI MEDICINA E CHIRURGIA

Dottorato di Ricerca in Fisiologia

Ciclo XXVIII

Tesi di Dottorato di Ricerca

ROS, pH and chloride currents as a virtuous (vicious?) loop in cell cycle progression of Glioblastoma Cancer Stem Cells

Dottorando: Dott. Marta Peretti

Matricola R10254

Tutor e Coordinatore: Prof. Michele Mazzanti

Dip. Bioscienze, Università degli Studi di Milano

Anno accademico 2014/2015

TABLE OF CONTENTS

1.ABSTRACT

The intracellular chloride channel 1 (CLIC1) is a peculiar metamorphic protein, belonging to a still partially unexplored family of chloride channels, that shuttles between a cytoplasmic and a transmembrane form, the latter able to form a chloride selective ion channel. Different factors regulate this membrane insertion, in particular an increase in the oxidative level and a modification in the pH. CLIC1 has been found to be overexpressed in different tumors, among the others in Glioblastoma Multiforme (GBM). GBM is the most lethal, aggressive and diffuse brain tumor. One of the clinical challenges of GBM treatment is to hit selectively its cancer stem cells (CSCs) that are responsible for tumor origin, progression and recurrence. CLIC1 protein, in its transmembrane form, has a pivotal role in the tumorigenic potential, proliferation and self-renewal of CSCs isolated from grade IV human GBM. CLIC1 could represent a suitable pharmacological target as the protein, physiologically located in the cytoplasm, is highly expressed in the plasma membrane only of glioblastoma CSCs enriched cultures. In a work published last year from our laboratory we have shown that blocking CLIC1 ionic current impairs specifically proliferation of CSCs and tumor development; moreover, we demonstrated a partial but significant arrest of cells in G1 phase after CLIC1 functional inhibition. Our experiments further demonstrate the great potential of CLIC1 as a pharmaceutical target since the functional expression of CLIC1 protein as a chloride ion channel occurs selectively in CSCs compared to Mesenchimal Stem Cells. My thesis work has been concentrated in the direction of uncovering the mechanism that regulates the protein expression in the plasma membrane of GBM cancer stem cells. My results have shown that CLIC1 membrane ionic current is differently tuned during the cell division process and its activity is fundamental for the progression of the cell cycle since the inhibition of CLIC1 transmembrane ionic flow causes a drastic reduction in the transition between G1 and S phase. Electrophysiology experiments showed that the chloride conductance mediated by CLIC1 in CSCs is increased at specific time points after the release from G1 synchronization of the cells. This tuning is regulated by an increase in the internal pH of CSCs that occurs during the progression of G1 phase of the cell cycle. Moreover, the last experiment set that I performed showed a regulation of CLIC1 chloride conductance during G1 phase also by

Reactive Oxygen Species (ROS) production by NADPH oxidase. Since both acute and chronic inhibition of CLIC1 channel activity with the specific inhibitor IAA94 leads to alteration in both internal pH and ROS levels I speculate a feed-forward mechanisms that links all these three elements that work synchronously to allow the progression through the cell cycle.

2.INTRODUCTION

2.1 Chloride channels and cancer

Over the last two decades an important role for ion channels in tumor developing and growth has been defined, so that they are currently included among the novel targets for cancer therapy. Channel dysfunctions may have a strong impact on cell physiology and signaling and it became clear that an abnormal triggering of ion channels activity could be important to support the high rate of proliferation of tumor cells. On behalf of this, ion channels expression is often altered in tumor cells; during the change from a physiological conditions towards neoplastic state a series of genetic alterations occurs, which may also affect the expression of ion channels or may cause a change in ion channel activity [8].

In the last years it has been confirmed the implication of ionic permeabilities in many aspects of cancer pathology, including uncontrolled growth, decreased apoptosis, disorganized angiogenesis, aggressive migration, invasion and metastasis [9]. A great number of studies in this field focused on the role of potassium channels but, with the flow of time, chloride channels gain more significance in this regulation [10].

Chloride channels are expressed ubiquitously and they reside both in the plasma membrane and in intracellular organelles. They have many different functions as the regulation of electrical excitability, transepithelial fluid transport, ion homeostasis, pH levels or cell volume regulation, the latter particularly important in cancer. Lately, it has been demonstrated that these channels have also a role in the regulation of the cell cycle progression, probably as a key factor for the progression from G1 to S phase. The different families of chloride channels display heterogeneous characteristics in the control of their activity. Specifically they can be voltage-activated, calcium-activated, ligand-activated, volume-activated or, in the case of cystic fibrosis transmembrane conductance regulator (CFTR), activated by cyclic AMP-dependent phosphorylation [11].

The intracellular chloride concentration is central to the activity of channels and transporters. As an example, the polarity of GABA responses depends upon it. In the immature brain, where the internal chloride concentration is high, the activation of GABA receptors promote a

depolarization. In contrast, in the adult brain, the amount of chloride inside the cell is lower, with consequent inhibitory action of $GABA_A$ergic currents [12].

Moreover, in the last years it has been shown that the cells use changes in intracellular chloride concentration to modulate many physiological functions, for example the regulation of mRNA expression of ion channels [13, 14], the activation of signaling molecules of the apoptotic pathway [14] or the release of prostaglandin [15].

Chloride currents have a role in the proliferation of many cell types like microglia, glioma cells, cells from neuroblastoma and endothelial cells [16-19]. In addition, as for K^+ channels, it has been observed a cell cycle-dependent expression of Cl^- channels. For example, ClC-5 expression in myeloid cells was high during S and G2/M and low in G0/G1[20]. In lymphocytes, chloride permeability also varied with the cell cycle, being low in G0 and S phase and high in G1/S [21]. The cell cycle-dependent expression of a glioma-specific chloride channel was linked to cytoskeletal rearrangements associated with cell division and cell swelling [22]. It is likely that, during proliferation, these channels balance transmembrane movement of ions and substrates and provide a mechanism for regulatory cell volume decrease (RVD) during cell cycling [8].

In light of these observations we can speculate that the internal chloride concentration could play an important role also in cancer cells, acting like a messenger to activate downstream pathways.

The literature offers us many examples of how chloride channels are involved in tumors development and progression. Members of the different families of chloride channels have been reported to have an active role in various tumors' progression. As an example, voltage-gated chloride channels, in particular CLC-3, CLC-2 and CLC-5 are involved in the regulation of cell volume needed for cells migration and invasion in glioblastoma [23]. CLC-3 in particular has a role also in other tumors like prostate cancer or nasopharyngeal carcinoma [24, 25].

In the last years, members of the intracellular chloride channels (CLICs) family, in particular CLCI1 and CLIC4, gained a more important role in tumors progression and development. As

the two channels have different patterns of expression in different tissues they also have different levels of expression in different tumors. The peculiarity of the channels belonging to this family, compared to “classical” membrane-resident chloride channels, is that their translocation and functional membrane insertion could be modulated in response to different stimuli like perturbation of cell homeostasis, making them a particular and very interesting pharmacological target [26].

2.2 Chloride intracellular channel 1 (CLIC1)

Among all the well characterized chloride channels, the chloride intracellular channel (CLIC) protein family has been the last discovered and still largely underexplored. These proteins are highly conserved in all vertebrates suggesting their involvement in basic biological functions. The first identified intracellular chloride channel, p64, was isolated from microsomes of bovine kidney and trachea and showed chloride selective channel function in lipid bilayers [27].

As mentioned above, distinct from membrane resident ion channels, these proteins can exist both as cytoplasmic soluble proteins as well as integral membrane elements with ion channel activity. Membrane insertion occurs in response to different stimuli from increases of cytoplasmic oxidation to pH changes [7, 28, 29].

CLIC1 and CLIC4 were the first CLIC proteins to be cloned and functionally studied [30, 31], and so far they remain the most characterized within the whole family.

CLIC1 was first cloned in 1997 from a human monocytic cell line. Firstly identified on the nuclear membranes, it was then localized also on the plasma membranes [30, 32]. This channel is highly conserved among the vertebrates, it is ubiquitously expressed in the different tissues and it is overexpressed in different tumors [26, 28].

2.2.1 Structure and biophysical properties

CLIC1 is a 241 amino acid protein with a molecular weight of 27 kDa. Being a metamorphic protein [33], it has different tertiary structures that correspond to the same primary sequence; it exists usually in a soluble form in the cytoplasm and nucleoplasm, but following different stimuli it undergoes major structural changes and inserts in lipid membranes where it acts as a chloride-selective ion channel [29, 34-36].

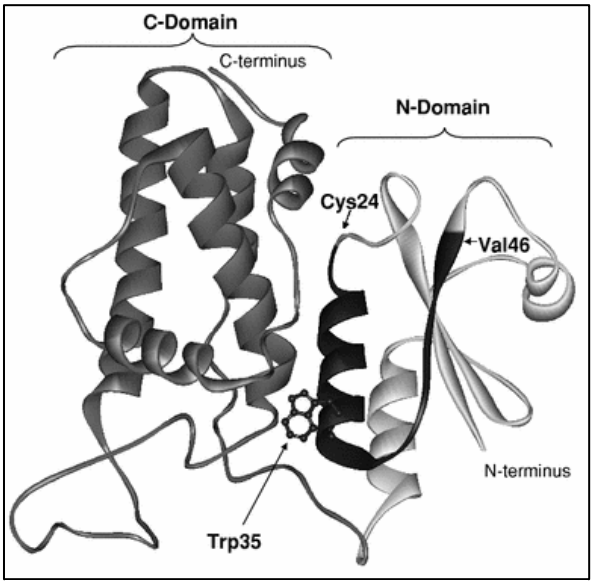

Figure 1: Crystal structure of CLIC1 monomer[6]

The structure of the soluble form of CLIC1 has been determined in two crystal forms at 1.4-Å and 1.75-Å resolution by Harrop and colleagues in 2001. This structure indicates that it is a homolog of the member of the GST superfamily. The N-domain (residues 1–90) has a thioredoxin fold that consists of a four-stranded mixed β-sheet plus three α-helices, while the C-domain is all helical, closely resembling the Ω class GST (Figure 1).

The N-domain has a well conserved glutaredoxin-like site for covalently interacting with GSH. Glutathione appears to be covalently attached to Cys^{24} via a disulfide bond, noncovalent binding of GSH to CLIC1 appears to be weak. In oxidizing conditions, glutathione detaches from its binding site and the N-terminal domain of the protein undergoes conformational rearrangements that expose hydrophobic regions that are able to interact with cellular membranes [37].

The crystal structure of the transmembrane form still has to be resolved. It has been postulated one putative transmembrane helix to form the membrane-spanning region of the CLIC1 module; it shows the length and the hydrophobic features necessary to spam the

plasma membrane. This region is localized between Cysteine 24 and Valine 46 and is located within the N-terminal domain.

In the structure of the monomeric soluble form of CLIC1, this putative segments forms a α helix and a β strand within the glutaredoxin-like-N-domain. Thus, in the transition from the hydrophilic to the membrane binding protein a large scale structural rearrangement, that may involve the N-domain of CLIC1 and disrupt the glutathione-binding site, is likely to occur [4, 7].

The structure of a dimeric, soluble, oxidized form of CLIC1 was resolved by Littler and colleagues in 2004 (Figure 2). In this form the glutaredoxine-like-N-domain has undergone a radical rearrangement to expose an extended hydrophobic surface, which forms the dimer interface. This transition, that is reversible on reducing conditions, is stabilized through the

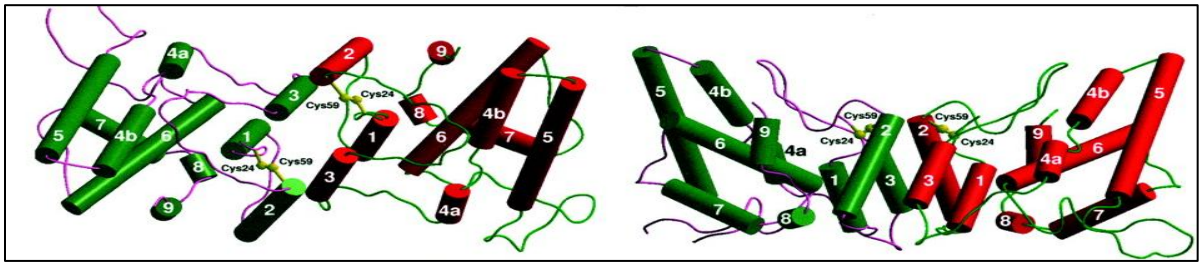

Figure 2: structure of the oxidized CLC1 dimer viewed along (left) and perpendicular (D) to the pseudo 2-fold axis[7]

formation of an intramolecular disulfide bond between two originally distant cysteine residues, Cys-24 and Cys-59. This dimer is able to form, in artificial lipid bilayers, chloride ion channels similar to the native channel. The mutation of either one of the two cysteine residues results in the loss of channel activity [7].

The mechanisms that allow CLIC1 membrane insertion still has to be fully elucidated. According to Littler model they suggest that the hydrophobic region exposed after the oxidation-dependent transition may represent the membrane docking interface.

Goodchild and colleagues performed experiments to clarify this membrane insertion mechanism. They suggested that the dimerization process is not necessary for the insertion of the protein into membranes. They propose a model in which at first there is a docking of monomeric CLIC1 to the membrane internal side and successively cytoplasmic oxidation promotes the structural changes that allow the protein to cross the membrane and form a

functional ion channel. They showed that both monomeric and dimeric forms are able to form functional ion channels in artificial membranes [6].

It has been demonstrated that, once inserted in the membrane, the protein exposes its N-terminus to the extracellular side, whereas the C-terminus remains on the intracellular side of the membrane [32].

Despite the fact that is still not clear how many subunits participates to form the functionally active structure, once inserted in the membrane, CLIC1 is able to act as a selective chloride channel; different hypothesis propose the association of two or four subunits, until the formation of small oligomers of six or eight subunits, to constitute one single ion channel [6, 28, 29, 32, 34, 35].

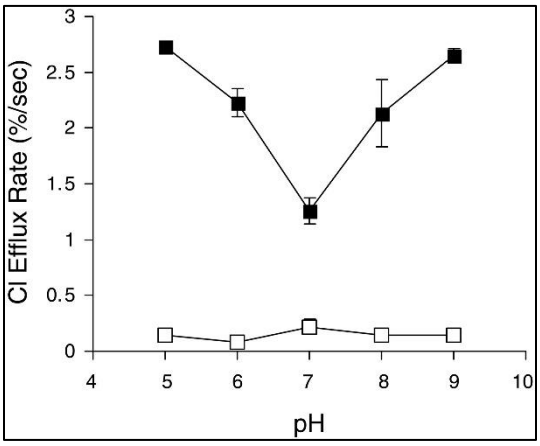

Figure 3: Effect on pH on CLIC1 activity in lipid bilayers[4]

Besides the oxidative level of the cytoplasm, as previously reported, the pH of the intracellular compartment plays a role in the regulation of CLIC1 membrane insertion. It has been demonstrated that in artificial lipid bilayers CLIC1 channel activity is dependent on H^+ ion concentration: it is minimal at pH 7 and it increases significantly with changes in the pH of the vesicles containing the protein (Figure 3) [4]. Recently it has been shown that, in particular, two histidine residues are fundamental or this pH-dependency [38].

Electrophysiological experiments performed on CHO cells transfected with a plasmid to overexpress CLIC1 allowed to understand the biophysical features of the channel. In physiological conditions, when the cells are at membrane voltages higher than the chloride reversal potential, CLIC1 mediates an outward current that rectified at +40/+50 mV. A small inward current is recorded at potential lower than the chloride reversal potential [32].

CLIC1 mediated current is completely and reversely blocked by the specific inhibitor IAA94 (Indanyloxyacetic acid 94), while the aspecific inhibitor of chloride channels DIDS (4,4'-Diisothiocyano-2,2'-stilbenedisulfonic acid) does not have an effect on CLIC1 conductance

[39]. A recent work published form our laboratory propose the antidiabetic drug metformin, that also has an antitumoral effect, as a selective blocker for CLIC1 channel activity [5].

2.2.2 Role in the pathology

Oxidation is one of the most important stimuli responsible for CLIC1 membrane colonization. Reactive Oxygen Species (ROS) may act as compounds that impair cell and protein function, but they may also act as second messengers in cellular processes that involve changes in the cellular redox state, including migration, differentiation, and cell replication. Indeed, many proteins have redox-sensitive motifs. Cell homeostatic mechanisms establish a balance between ROS production and their removal by antioxidant systems. The overwhelming of antioxidant defenses by ROS generation results in a condition of oxidative stress. Several pathological conditions are characterized by changes in cellular redox state, in particular chronic inflammatory states, oncologic conditions [40] and degenerative process [41-43]. Concerning CLIC1 role in diseases, it has been observed an involvement of the membrane protein during tumor proliferation or in neurodegenerative processes [44-46]; these two pathological states share the common feature of an overproduction of ROS. The hypothesis that CLIC1, in its channel form, could play a role in the pathophysiology of these conditions promotes the protein as a potential valid therapeutic target.

Alzheimer's diseases (AD) is characterized by an activation of the microglia induced by β amyloid (Aβ). Once the microglia is activated is highly proliferating and it produces a large amount of ROS due to the activity of membrane NADPH (Nicotinamide Adenine Dinucleotide Phosphate) oxidase. Our laboratory has shown that in microglia stimulated by Aβ, CLIC1 is over-expressed [44]. The blockade of CLIC1 functional expression limits the detrimental effects due to the over-activation of microglia cells, impairing the production of TNF-α, nitrites and ROS [45]. The hypothesis about the role of CLIC1 during ROS hyper-production is linked to the fact that NADPH oxidase function is strictly dependent on the membrane potential, since depolarized voltages limit its activity. Hence, CLIC1 could have a role as a "charge compensator" to maintain hyperpolarized membrane voltages and sustain NADPH oxidase activity. In this way, not only CLIC1 membrane translocation is promoted by an increase in

ROS production, but also ROS production is supported by the chloride current mediated by CLIC1 channel [45].

Concerning CLIC1 and its expression in cancers, the protein levels are reportedly increased in human breast ductal carcinoma [47], gastric cancer [48], gallbladder metastasis [49], colorectal cancer [50], nasopharyngeal carcinoma [51], ovarian cancer [52], hepatocellular carcinoma [53] and high-grade gliomas [54]. All these reports propose CLIC1 as a tumor marker, sometimes detectable even in the plasma of patients and so very useful in the clinic.

It is known that oxidative level oscillations in the intracellular compartment contributes to the regulation of cell cycle progression through the different phases [55] and that alterations in the oxidative basal level of the cells are typical conditions for many tumorigenic processes. It is not surprisingly so that the activity of CLIC1 channel, induced by the oxidation, is higher in hyper-proliferating tumor cells. Like activated microglia, cancer cells could also take advantage of a feed-forward mechanisms between CLIC1 channel activity and ROS production.

The fact that, in prolonged stress conditions, CLIC1 membrane expression becomes no more transient but chronic makes the channel a very interesting potential pharmacological target, making possible to hit specifically cancer cells. This will limit the toxicity due to the unspecific targets often choose in conventional antitumor therapies [26].

2.3 Glioblastoma multiforme and cancer stem cells

2.3.1 Gliomas

Gliomas are the most common group of primary brain tumors characterized by high malignancy and invasiveness; each year, about 5–6 cases out of 100,000 people are diagnosed with primary malignant brain tumors, of which about 80% are malignant gliomas [56, 57]. These tumors took their name from the fact that they originates from neoplastic transformation of mature glial cells, especially astrocytes, oligodendrocytes or ependymal cells, or their precursors [58]. Gliomas include astrocytomas, oligodendrogliomas and

ependymomas. Malignant gliomas are subcategorized according to World Health Organization (WHO) into grade III tumors, such as anaplastic astrocytoma, anaplastic oligodendroglioma, anaplastic oligoastrocytoma and anaplastic ependymoma, as well as grade IV tumors, as glioblastoma multiforme (GBM), the most aggressive and lethal among the brain tumors. The WHO grade is assigned based on certain pathological features, such as nuclear atypia, mitotic activity, vascular proliferation, necrosis, proliferative potential, clinical course and treatment outcome [59]. Grade III and IV gliomas are characterized by necrosis and anaplastic cells that are able to hyper-proliferate and to infiltrate in the brain parenchyma. Lower grade gliomas (I and II) are made of cells that are still differentiated, histologically similar to astrocytes and oligodendrocytes, they are mostly benign and with a better prognosis compared to higher grade gliomas [3, 60]. However, the fate of most low-grade gliomas is to undergo malignant transformation over the years

The diagnosis of brain tumors is performed by magnetic resonance imaging (MRI) and the use of adjunct technology such as functional MRI, diffusion-weighted imaging, diffusion tensor imaging, dynamic contrast-enhanced MRI, perfusion imaging, proton magnetic resonance spectroscopy and positron-emission tomography to define localization, dimensions and grade of the lesion. Anyway, it always has to be confirmed with a biopsy of the tumor mass. Clinically, patients with GBM may present with headaches, focal neurologic deficits, confusion, memory loss, personality changes or with seizures [61].

The mean age for the diagnosis of gliomas is 64 years. Its incidence in the United States is estimated around 3:100,000 while more than 10,000 cases are diagnosed annually; incidence has increased slightly over the past 20 years, mostly due to improved radiologic diagnosis, and especially in elderly. This tumors are 1.5 times more common in men than women and 2 times more common in Caucasians compared to Afro- Americans [57].

Nowadays, the gold standard of care in patients younger than 70 years old provides for maximal surgical resection plus radiotherapy plus concomitant and adjuvant temozolomide or carmustin administration. Unfortunately, despite the treatment, recurrence is likely to overcome and the great majority of the patients will die in two years from the diagnosis [56].

The biggest problems in the treatment of GBM are mainly the wide heterogeneity inter and intra-tumors, the high infiltration rate and the complexity for the therapeutic agents to cross the blood brain barrier and to hit selectively GBM cancer stem cells (CSCs), that are responsible for the tumor origin, progression and recurrence and that will be described deeply in the next paragraph.

Concerning the genetic alteration of gliomas, there are some altered oncogenes and tumour-suppressor genes involved in these pathologies. These mutations are not specific of brain tumors, however their combination and accumulation are characteristic. One of the earliest genetic modification in low-grade astrocytomas is the overexpression of platelet-derived growth factor (PDGF) ligands and receptors that cause an autocrine growth-factor stimulation loop and inactivation of the TP53 gene. Since the TP53 gene has several functions including to induce cell-cycle arrest (at the G1/S and G2/M transition points), DNA repair, apoptosis or their combination in response to genotoxic stress, its inactivation promotes abnormal cell division and seems to facilitate anaplastic transformation through genomic instability. In addition to TP53 mutation, the tumors have accumulated other genetic alterations, particularly those implicated in the retinoblastoma- mediated cell-cycle regulatory pathway eventually leading to an uncontrolled progression of the cell cycle from the G1 to the S phase. Moreover, a characteristic of primary malignant gliomas, especially glioblastomas, is amplification and overexpression of epidermal growth factor (EGF) receptor (>50% of cases). As for PDGF receptor, activation of EGF receptor induces downstream signal transduction pathways producing cellular proliferation and invasiveness. The retinoblastoma pathway is also altered in most primary malignant astrocytomas [60] [62]. Thus, gliomagenesis and tumor progression are closely associated with loss of cell cycle control and increased tyrosine-kinase signaling. At a late stage of tumor progression these pathways are involved in essentially all malignant gliomas and are linked together [60].

In murine genetic models in which genes are introduced or removed at the germline (transgenic or knockout mice) or somatic levels (eg, gene transfer using retroviral vectors),

there is strong evidence of a causal role of the dysregulation of these pathways in glioma formation [3].

Glioblastoma multiforme (GBM) is the most aggressive and lethal brain tumor; in the United States 54% of all gliomas are classified as GMB (Figure 4) and the median survival after the diagnosis varies from 6 months to 2 years; the five years survival rate is less than 3% [63].

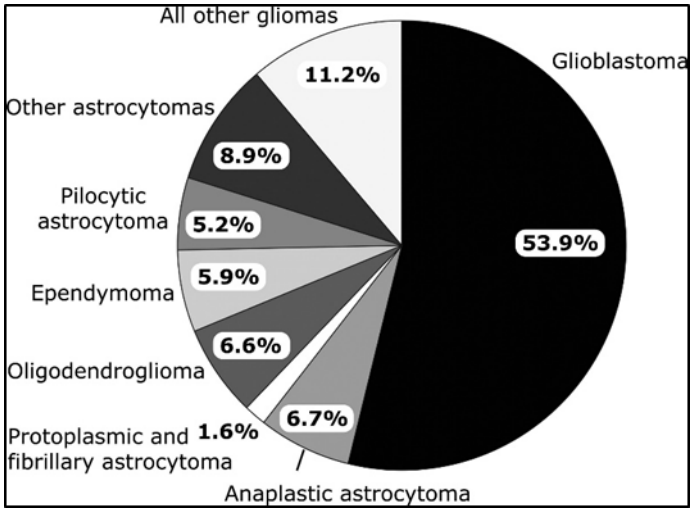

Figure 4: frequency of primary CNS gliomas in the United States from 2004 to 2006[3]

Glioblastomas might develop *de novo* (primary glioblastoma) or through progression from low-grade or anaplastic astrocytomas (secondary glioblastoma). Primary GBMs account for a great majority of cases in older patients, while secondary GBMs are quite rare and tend to occur in patients below the age of 45 years. Primary GBMs present in an acute de novo manner with no evidence of prior symptoms or antecedent lower grade pathology. In contrast, secondary GBMs derive consistently from the progressive transformation of lower grade astrocytomas, with 70% of grade II gliomas transforming into grade III/IV disease within 5–10 years of diagnosis. Remarkably, despite their distinct clinical histories, primary and secondary GBMs are morphologically and clinically indistinguishable as reflected by an equally poor prognosis when adjusted for patient age. However, although these GBM subtypes achieve a common phenotypic endpoint, recent genomic profiles have revealed strikingly different transcriptional patterns and recurrent DNA copy number aberrations between primary and secondary GBM as well as new disease subclasses within each category [63].

Initially it was considered that glioblastoma arose from astrocytic precursors and was genetically characterized by amplification of EGFR and expression of glial fibrillary acidic protein (GFAP). GFAP is highly specific for cells with astrocytic differentiation and is widely used as a reliable marker in immunohistochemical diagnosis and differentiation of brain

tumors including glioblastoma [64]. In the last years however, many evidences have suggested that tumor organization could be described similarly to the hierarchy of stem cells and various progenitor cells that are locally restricted to the stem cell niche. Demonstrations that the adult human forebrain contains an abundant source of neural stem cells (NSCs) and that human GBMs contain tumorigenic neural stem-like cells indicate that neural stem and/or progenitor cells are a plausible origin for human gliomas and have given rise to speculations that more effective therapies will result from targeting stem cell-like component of GBMs [65, 66].

2.3.2 Brain tumor Cancer Stem Cells

Historically, a stem cell is defined as an "undifferentiated cell capable of proliferation, self-maintenance, production of a large number of differentiated functional progeny, regenerating the tissue after injury and flexible in the use of these options" [67]. Stem cells are undifferentiated cells able to generate every type of mature cells present in their tissue of origin (multipotency) and, at the same time, to maintain a constant pool of stem cells for the entire life of the individual (self-renewal) [1, 67]. Stem cells can accomplish self-renewal in two possible way; either undergoing asymmetrical divisions, by which are generated both a faithful copy of the mother cell and a mature progenitor, or symmetrical division, by which are generated either two stem cells or two mature progenitors. The self-renewal capacity is the best feature to distinguish between somatic stem cells and their immediate descendants that are only able to reproduce themselves in a limited fashion. An alteration in the regulatory mechanisms that control self-renewal are probably involved in the genesis of cancer-initiating stem-like cells [1].

The heterogeneity of tumor cells has long been appreciated, but only in 1997 a work from Dick's laboratory described the isolation of a leukemia-initiating cell, the first purification of cancer stem-like cells, a population that had originally been proposed to exist more than 150 years earlier [68]. In the next years brain Cancer Stem Cells (CSCs) have been described in anaplastic astrocytoma, medulloblastoma, pilocytic astrocytoma, ependymoma, ganglioglioma and GBM [65, 69-71]. These brain CSCs have subsequently been shown to

be resistant to standard-of-care chemotherapy [72] and radiotherapy [73], underscoring their role in disease progression and recurrence.

Regarding the origin of these CSCs there is evidence that multiple cell types, from stem cell to differentiated progeny, are amenable to oncogenic transformation. Therefore it is essential that the strictest functional assays continue to be performed. As the accepted functional definition of a stem cell is the ability to self-renew and generate differentiated progeny, also the cancer stem cells should be defined as a cell able of self-renewal, originating new malignant stem cells and, at the same time, capable to differentiate in every non-tumorigenic cell types present in the primary tumor [74]. CSCs are also described as a tumor subpopulation which can be self-renewed in vitro. Moreover, they are able to regenerate the tumor after orthotopic transplant in vivo and to originate all the tumor progeny both in vivo and in vitro [75]. As an examples, brain cancer stem cells have the ability to generate, upon intracranial transplantation, a tumor that recapitulates the cellular heterogeneity present in the parental tumor.

Cancer arises from a series of mutations that occurs in few or even single founder cells, these cells eventually acquire unlimited and uncontrolled proliferation potential. This phenomenon could be explained by two hypothetical models: the stochastic or the hierarchical model (Figure 5). The first one predicts that all the cells in a tumor have a similar tumorigenic potential, activated asynchronously and at low frequency in certain cells. On the other hand, the hierarchical model claims that only a rare subset of cells within the tumor have significant proliferation capacity and the ability to generate new tumors, while the other bulk cells are differentiating or terminally differentiated cells. This second hypothesis fits with the cancer stem cell theory and, in the last years, is the most supported [1, 76]. Actually, it has to be

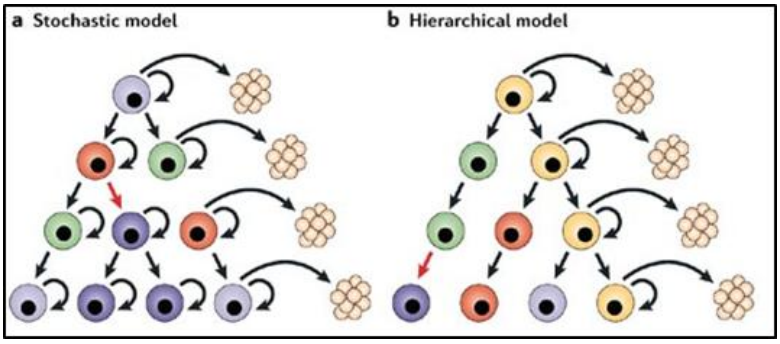

Figure 5: stochastic and hierarchical models of tumors initiation and development [1]

pointed out that the CSC could be distinguished from the Tumor Initiating Cell (TIC), which is the first cell tumorigenically transformed and responsible for the origin of the tumor. As mentioned above, it has been recently demonstrated that a CSC do not necessarily derive from the transformation of a normal stem cell but it could originate from a more differentiated progenitor capable of self-renewing [74, 75, 77].

Regarding brain tumors, the identification of the cellular origin of glioma is a great opportunity to improve the knowledge of the disease. Until the end of the 1990s there was the belief that, in an adult brain, mature glia was the only dividing cellular population and so that the neoplastic transformation of mature glia or the dedifferentiation of adult glial cells could be the only way for the gliomagenesis. In the last two decades a number of studies discovered and isolated other cellular populations in the brain able to proliferate, self-renew and originate neurons and mature glia after damage: neural stem cells and glial progenitor. The main implication of continued adult neurogenesis is the presence of these undifferentiated, mitotically active stem and progenitor cells within discrete regions of the mature brain. Like for the other tissues, these populations might function as a source of cells for transformation, giving rise to tumor stem cells [1].

Neural stem cells can be isolated and expanded in cell culture depleted of serum and enriched with EGF (Epidermal Growth Factor) and FGF2 (Fibroblast Growth Factor 2). In this selective culture, partially differentiated cells died while neural stem cells rapidly divide in response to mitogen stimuli and form neurospheres in suspension that can be dissociated and re-plated to generate secondary spheres. The process can be repeated, resulting in a geometric expansion in the number of cells that are generated at each passage. Upon mitogen removal, the progeny of the proliferating precursor can be differentiated into neurons, astrocytes and oligodendrocytes, which are the three primary cell types found in adult mammalian central nervous system. This neurospheres assay allows to study the proliferative potential of stem cells populations and so is used to isolate, expand and identify neural stem cells, with multipotency and self-renewal ability [1].

The same assay is performed also to isolate, amplify and identify brain cancer stem cells (Figure 6). When these cells are plated in absence of mitogens they differentiate into the different cellular types that compose the tumor. With this assay, the presence of cancer stem cells is valuable only retrospectively; furthermore, if associated with in vivo tumorigenicity assays, it is used to confirm that the supposed cancer stem cell really is a tumor initiating cell [1, 78, 79].

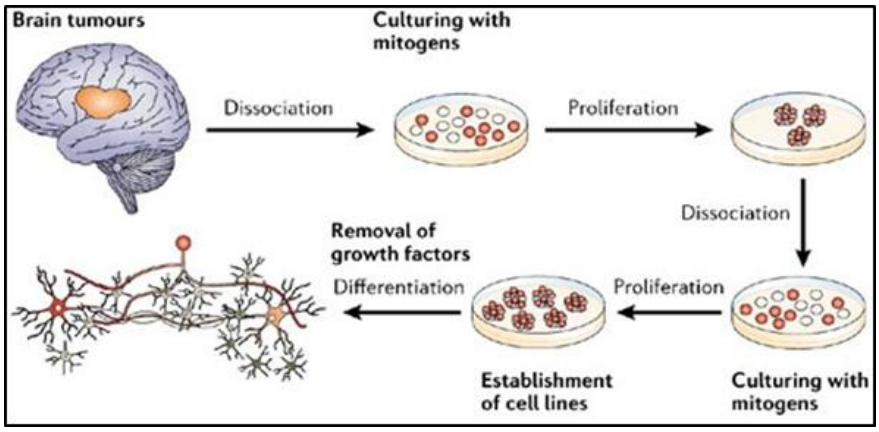

Figure 6: Isolation and perpetuation of brain tumor stem cells in culture [1]

Most glioma CSC markers have been appropriated from normal stem cells, but the link between glioma CSCs and normal stem cells remains controversial. Many of the transcription factors or structural proteins essential for normal neural stem cells function also mark glioma CSCs, including SOX2 [70], NANOG [80], OLIG2 [81], MYC [82], MUSASHI1, BMI1 [70], NESTIN [83] and inhibitor of differentiation protein 1 (ID1) [84]. However, because of the limited utility of intracellular proteins to enrich CSCs from non-stem tumor cells (NSTCs) using traditional methods such as flow cytometry, a multitude of potential cell surface markers have been suggested including CD133 [70], CD15 [85], integrin α6 [76], CD44 [86], L1CAM [87] and A2B5 [88]. These types of cell surface markers mediate interactions between cells and the microenvironment. Dissociation of cells from their surroundings rapidly degrades the informational content of markers, requiring rapid utilization.

Although CD133 continues to be the most commonly used cell surface marker, other markers, such as integrin α6, have been proposed to segregate CSCs and NSTCs [89]. CD15/SSEA-1 and CD44 have also been proposed as possible markers, potentially in association with specific subgroups of GBM [90]. These markers are useful but they must be approached with caution. Each of them is able to interact with a large percentage of cells, consistent with a high false-positive rate. However it is likely that no marker will ever be

uniformly informative for CSCs: most tissue types contain multiple populations of stem cells expressing different markers and, in addition, for the inherent adaptability of cancer cells. Thus, several methods other than marker expression have been used to enrich glioma cell population with CSCs, such as the neurosphere assay.

An alternative approach to CSC enrichment, which is based on the hypothesis that stem cells contain drug efflux transporters [91], is the use of flow cytometry to isolate a side population containing CSCs. While this approach has identified a population of self-renewing cells in a mouse glioma model, it has not been used successfully to enrich for self-renewing cells in human GBM [92, 93], highlighting the model- and species-specific challenges of enrichment methods.

Therapeutically speaking, the discovery of brain cancer stem cells has two major implication: the cancer stem cells, which contain all the genetic information to faithfully reproduce the original tumor, can be used as a model to look for new diagnostic markers and for screenings of potential drugs; moreover, therapies directed specifically against CSCs could give better clinical outcomes (Figure 7). The great clinical challenge of GBM treatment is probably strictly connected to the existence of CSCs that are usually not the target of classical surgery or pharmacological treatments, which are normally directed against highly proliferating but not tumorigenic cells. CSCs, usually quiescent and with a high expression of anti-apoptotic proteins and drug efflux transporters are the reservoir for a potential tumor recurrence [1].

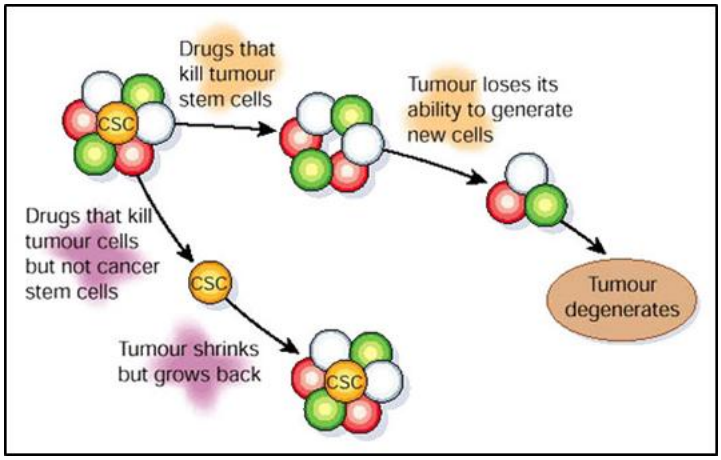

Figure 7 : Comparison between conventional antitumoral therapy and a hypothetical therapy that hits specifically CSCs [2]

2.4 CLIC1 and glioblastoma

An important role for CLIC1 as a chloride channel is specifically associated with the development of glioblastoma. CLIC1 is highly expressed in glioblastoma and both mRNA and protein levels are increased in high grade in comparison to low grade brain tumors or control (non-tumor) brain tissue [46, 54]. Upon CLIC1 silencing, both proliferative capacity and self-renewal properties in vitro were impaired. Moreover, immunodeficient mice injected into the nucleus caudatus with CLIC1-silenced CSCs, survived longer than non-treated CSCs-injected control mice [46]. However, RNA interference experiments per se are not able to distinguish whether CLIC1 is active as a cytoplasmic component or if the ability to modulate CSCs proliferation and migration is due to its plasma membrane ion channel property. To address this specific task, Setti and co-workers [46] showed not only that the IAA94-sensitive membrane current was drastically reduced in CLIC1 silenced human glioma CSCs, but also that CSC neurospheres, treated for 48 h with NH2-CLIC1 antibody, active as a CLIC1 channel blocker only from outside the cell [32], compromised cancer development in injected mice. Angelini and colleagues [26] calculated the ratio between CLIC1-mediated current and other Cl^- currents obtained from perforated-patch experiments in CSCs isolated from four different human glioblastoma postsurgical specimens. The relative large amount of CLIC1-mediated current positively correlates with tumor aggressiveness. These results support the idea that the abundance of CLIC1 protein in the plasma membrane is a precise sign of a cell in unbalanced condition. This condition could be a transient event in a regular function of the cell life. However, if the protein overexpression becomes chronic as in glioblastoma CSCs, CLIC1 activity could be instrumental to the progress of the pathological state. More important, if the modulatory action is represented by the chloride ion channel, CLIC1 could be considered a privileged therapeutic target for CSCs in glioblastoma as well as in other untreatable tumors. A recent report from our laboratory strongly supported this hypothesis showing that CLIC1 activity can be pharmacologically regulated, discriminating among CSCs and normal stem cells. The inhibitory effect of both IAA94 and Metformin on proliferation was shown to be evident only in glioblastoma CSC-enriched cultures, while when the same

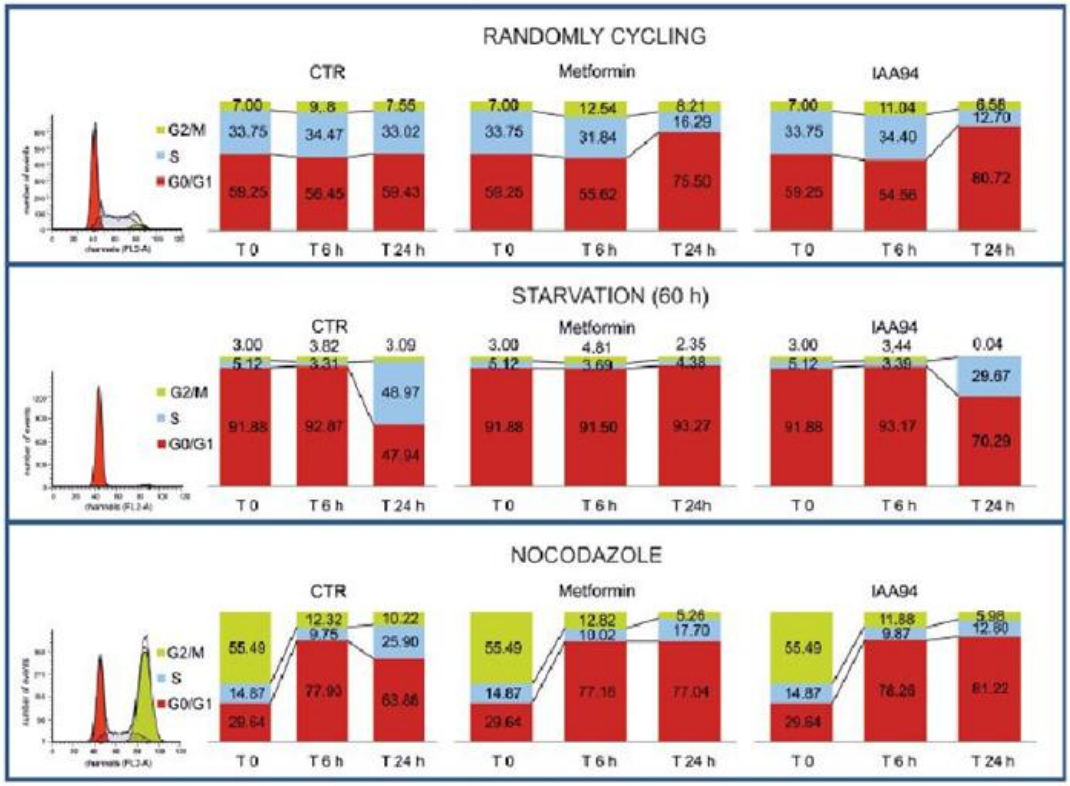

Figure 8: effect of CLIC1 blockage with Metformin or IAA94 on the progression of cell cycle [5]

cultures were differentiated through a switch in the culture medium, they were unaffected. Moreover, in light of the proposed role of CLIC1 over-activation in glioblastoma cells , in differentiated cells, that are not sensitive to the antiproliferative effects of the membrane protein inhibition , CLIC1 was mainly confined to a cytosolic localization in an inactive form not reachable by the inhibitors [5]. These results strongly support the potential role of CLIC1 as a pharmacological target that allows the discrimination between normal and tumor cells, especially in glioblastoma. In the same article, we reported also that the inhibition of CLIC1 current leads to significant accumulation of CSCs in G1 phase of the cell cycle, suggesting a role for the channel in the progression of the cell cycle (Figure 8).

2.5 pH and ROS in cell cycle progression and cancer

2.5.1 pH

Intracellular pH is fundamental for the activity of many enzymes, for the efficiency of contractile elements and for the conductivity of ion channels. Moreover, pH oscillations seem to be important in controlling the cell cycle and the proliferative capacity of cells.

Regarding the enzymatic activity, an important example of pH sensitivity is phosphofructokinase, the rate-limiting enzyme of glycolysis, which activity increases with increasing pH in the physiological range [94]. Furthermore, protein, DNA and RNA synthesis are affected by internal pH levels; as an example, the pH optimum of DNA polymerases activity is generally quite high; it is reported to increase with increasing pH from 7.0 to 8.0 [95].

Thus, in general, the metabolic activities of cells raises with raising internal pH.

Oscillations in intracellular pH have been shown to be important in the control of the cell cycle and cell division in both prokaryotic and eukaryotic cell type. A rapid increase in intracellular pH may be important to bring cells from G0/G1 into S phase [95].

A work of Gerson and colleagues, showed a biphasic increase in pH_i when lymphocytes were stimulated with the mitogen concanavalin A. The first peak was seen after 6-8 hours and the second peak 48 hours after the stimulation. While the first one correlated with early events, like the increase of phospholipids and protein synthesis, the second peak correlated with the synthesis of DNA [95].

Several works reported different evidences about pH regulation of the cell cycle progression. One of the leading hypothesis is that, possibly, a pH_i increase is necessary for the transition of cells from G0 to G1 in order to bring quiescent cells back into the cell cycle. Two works merged in this hypothesis; on one hand Pouyssegur reported that in response to growth factors, quiescent fibroblast mutants lacking the Na^+/H^+ exchanger activity failed to elevate their internal pH and to reinitiate DNA synthesis. On the other hand, Mills observed that

inducing proliferation in lymphocytes with interleukin 2 stimulates the Na^+/H^+ exchanger activity but if this exchanger was inhibited, proliferation occurred anyway [96] [97].

In the last decades it became more clear that maintaining a higher intracellular pH, associated with a more acidic extracellular space, is very important in the processes of neoplastic transformation and of tumoral progression. It seems that many typical features of a tumorigenic cells could derive from an alteration of the severe mechanisms that control internal pH. As an example, high cytoplasmatic pH could promote metabolic processes correlated with the cellular proliferation, while an extracellular acidification could increase the invasiveness of transformed cells [98] [99]. In this aberrant regulation of hydrogen ions dynamics an important role is played by the isoform 1 of the Na^+/H^+ exchanger, NHE. In cancer cells the NHE1 is hyperactive also in basal condition, leading to an alkalinization of the intracellular space that correlates with the uncontrolled proliferation typical of transformed cells [99]. It has been demonstrated that NHE1 has a role in in the regulation of the actin cytoskeleton dynamics necessary for the adhesion and pseudopodial protrusion of motile, invasive tumor cells [98].

The Na^+/H^+ exchanger is an antiport firstly identified in brush borders of rabbit kidney and small intestine [100]. It responds to a fall in extracellular pH by quickly extruding protons in exchange with extracellular Na^+. The energy for the extrusion is provided by the large inward-directed Na^+ gradient [95]. The NHE is inhibited by the potassium-saving diuretic drug amiloride and its analogues. Amiloride inhibits the exchanger competitively binding to the extra-cellular site which accommodates Na^+ ions. The antiport is also downregulated by the inhibition of the Na^+/ K^+ ATPase as well as the exposure of the cells to an external solution depleted of sodium [101] both action that dissipate the sodium gradient which drives the process.

Amiloride is a less selective and more toxic inhibitor compared to more specific analogues like Cariporide or EIPA (ethylisopropylamiloride).

An accumulation of protons in the cytoplasm could act as an allosteric activator of the exchanger as well as the exposure to the compound FMLP (N-Formyl-L-methionyl-L-leucyl-L-phenylalanine) [101].

Usually, the activity of NHE is low and balances the passive H^+ influx and the production of intracellular acidic metabolites; however, in specific condition, the activity of the exchanger could mediate a massive proton efflux, leading to an alkalinization of the intracellular compartment [95, 102].

Oncogene-driven neoplastic transformation constitutively activates NHE1 and raises pH_i by increasing the affinity of the allosteric proton regulatory site which mimics the lowering of cytosolic pH. Further, in a study to determine the mechanism of tumor cell activation by serum removal it has been demonstrated that this treatment stimulated NHE1 activity specifically in tumor cells though a PI3K-dependent increase of the affinity of this allosteric site.

The activity of NHE1 in tumor cells has often been associated with the activity of bicarbonate transporting systems. The effect of this hyper activation can bring the cytoplasmic pH of cancer cells to values of 7,8. Interestingly, although in MCF-7 has been reported that both transporters contributed to regulate pH_i, only the NHE1 played a role in regulating either motility or response to cisplatin chemotherapy [103].

2.5.2 ROS

Cellular proliferation encompasses tightly regulated biochemical and genetic pathways, the loss of which can lead to aberrant proliferation. In recent years, the role of the intracellular redox state as a growth regulator is increasingly becoming appreciated [104, 105]. Cellular redox state is a delicate balance between the levels of reactive oxygen species (ROS) produced during metabolism and the antioxidant system that scavenges them. ROS, including superoxide (O2·), hydrogen peroxide (H2O2) and hydroxyl radical (HO·) are known to inhibit activities of various biological molecules. However, at the end of the ‘90s , low levels of ROS have been recognized to serve as second messengers for signal transduction [106, 107].

In general, ROS contain one or more unpaired electrons in their highest occupied orbital. The partial reduction of molecular oxygen results in the production of superoxide ($O_2\cdot$) and hydrogen peroxide (H2O2). $O_2\cdot$ and H_2O_2 react with transition metal ions (e.g. cuprous and ferrous ions) through Fenton and Haber–Weiss chemistry, promoting further radical generation, including the highly reactive hydroxyl radical ($HO\cdot$) [108].

Cells can generate ROS from exogenous sources as well as endogenously. In the cytoplasm ROS are largely produced as oxidative by-products of cellular metabolism; mitochondria are the major site of $O_2\cdot$ production. Other endogenous sources of ROS include the superoxide-generating nicotinamide adenine dinucleotide phosphate (reduced form) (NADPH) oxidase complex, peroxisomes, metabolism of fatty acid chains, cytochrome P450 reductase, xanthine oxidase, myeloperoxidase and nitric oxide synthase [109-113].

To minimize the production of $HO\cdot$, H_2O_2 levels are tightly controlled by several enzymes, including catalase, glutathione peroxidase, thioredoxin and peroxiredoxins. Cysteine, GSH, vitamins C and E (ascorbic acid and a-tocopherol), among others, constitute a pool of small molecular weight non-enzymatic antioxidants [106, 114-117].

As mentioned above, the cellular response to small changes in the ROS concentrations can have beneficial effects on cell growth and viability while higher concentration of these ROS caused toxicity and reduced cell number, so that, in the last decades, it has been delineated a biphasic effect of these compounds [118].

Regarding cell cycle regulation, the first evidence of a redox cycle within the cell cycle came in 1931 from Rapkine [119] who demonstrated using sea urchin eggs the presence of soluble thiols that fluctuated cyclically. Later, Mauro et al., using synchronous HeLa cells, further dissected the changes occurring in protein-bound and non-protein sulfhydryl (–SH) and disulfide (–SS–) groups in each phase of the cell cycle [120]. Also budding yeast exhibits a metabolic redox cycle consisting of a reductive non-respiratory phase and an oxidative respiratory phase. Many of the genes regulating DNA replication and cell cycle progression are expressed during its reductive phase with cell cycle initiation occurring very late during the oxidative phase [121]. Menon and colleagues have shown previously that a transient

increase in prooxidant levels early in G1 is required for the cells to transit from G1 into the S phase, suggesting that an oxidative burst is required to proceed through G1 phase [55]. Moreover, reports from other laboratories have shown that sub–lethal doses of ROS ($O_2\cdot$ and H_2O_2) added exogenously stimulated proliferation in cultured hamster fibroblasts [105, 122]. Observation by Conour et al. indicates GSH content was significantly higher in the G2/M phase compared to G1, suggesting that cells in the G2/M phase are at a more reduced state compared to the G1 phase. S-phase cells showed an intermediate redox state [123]. The hypothesis of a redox cycle regulating the cell cycle is also supported by reports of antioxidant enzymes influencing cellular growth stage [124]. Moreover, it has been reported a redox regulation of the cell-cycle–regulatory proteins that could be influenced by the presence of redox-sensitive motifs, such as cysteine residues or metal cofactors in kinases and phosphatases [125].

This periodicity in intracellular redox state require a delicate balance between production of ROS and subsequent removal by antioxidants (both non-enzymatic and enzymatic pathways). Therefore, defects in ROS production and their removal could perturb the redox cycle, which in turn could lead to aberrant proliferation. Many of the proliferative disorders typical of pathophysiological conditions like cancer or neurodegeneration, are also associated with defects in the antioxidant pathways, presumably affecting redox regulation of cellular proliferation [126].

Aberrant proliferation in cancer cells could be due to a loss in the redox regulation of the cell cycle. This was first reported by Oberley and Buettner[127] who showed that cancer cells exhibit lower levels of antioxidant enzyme activities compared with their respective normal cells, in particular MnSOD. Later on, other studies were published suggesting that oxidative stress could significantly contribute to cancer progression, possibly by perturbing the redox control of the cell cycle. Redox potential in normal cells correlates with Rb phosphorylation status during the cell cycle, proposing that perturbations in cellular redox potential could significantly affect the function of a tumor-suppressor gene [125]. Moreover, in response to the activation of many oncogenes (Ras, Raf, Myc, Bcr–Abl, ERB2, etc), the unconstrained

mitogenic signaling enhances the production of ROS. ROS and redox signaling have impacts on origin licensing, initiation of DNA synthesis, and/or replication fork travel, thereby inducing replication stress and the DNA-damage response, the mechanisms of this regulation still have to be fully elucidated [128].

Furthermore, it is hypothesized that the metabolic redox-signaling pathways could initiate as well as promote carcinogenesis. This hypothesis is based on numerous studies demonstrating a regulatory role of MnSOD activity in cancer cell growth in both cell-culture and tumor xenograft animal model systems [125].

2.6 pH regulation and ROS production in glioblastoma

Malignant gliomas show an intracellular pH (pH_i) more alkaline and an extracellular pH more acidic compared to non-transformed astrocytes, despite their increased protons production [129]. To maintain an optimal pH_i, glial tumors must possess an efficient means of removing the excess H^+ produced as a result of their increased metabolism. The first evidences about which were the principal mechanisms responsible for intracellular pH regulation in gliomas cell lines have been obtained in 1994 by Shrode and Putnam. They demonstrated that in C6 rat glioma cell line the Na^+/H^+ exchanger NHE and the Cl^-/HCO^{3-} exchanger were active while the Na^+/HCO^{3-} cotransporter was absent [130].

Lately, McLean and colleagues demonstrated that three human glioma cell lines and one rat glioma cell line have an increased internal pH (0,3-0,5 unitis above pH_i of normal astrocytes). Moreover they also demonstrated that these cells lines rely primarily on the Na^+/H^+ exchanger to maintain their alkaline pH_i, whereas nontransformed astrocytes are able to maintain a constant pH_i even in the absence of NHE activity. The elevated steady-state pH_i of these glial tumors is not the result of genetic alterations of the NHE1 gene but is dependent upon an increased activity of this exchanger [131].

NADPH oxidase, as previously told, is one of the sources of endogenous ROS production. It can exist in four different isoforms: NOX1, NOX2, NOX3 and NOX4.

Shono and colleagues a few years ago showed that gliomas prominently express Nox4 transcript and protein and that the expression levels of Nox4 mRNA in GBMs (WHO grade IV) were significantly higher than those in other astrocytomas (WHO grade II and III). Moreover, in glioma cell lines the specific knockdown of this isoform leads to reduced expressions of some antiapoptotic genes and cell growth related genes and brings in morphological changes including a reduced cell size and multiple cytoplasmic processes [132].

Some years later it has been demonstrated that Nox4 is essential for cycling hypoxia-induced ROS production in GBM cells. Cycling hypoxia is a well-recognized phenomenon within animal and human solid tumors. It mediates tumor progression and radiotherapy resistance through mechanisms that involve reactive oxygen species production [133].

The same laboratory, in a following study, demonstrated that the cycling hypoxic tumor cells derived from glioblastoma xenografts have much higher Nox4 expression, NADPH oxidase activity, ROS levels and radioresistance than chronic hypoxic cells or normoxic cells. Moreover, Nox4 blockade in intracerebral glioblastoma-bearing mice decreased tumor microenvironment induced Nox4 expression and radioresistance, and further increased the overall therapeutic efficiency of radiotherapy [134].

3.MATERIALS AND METHODS

3.1 Human Glioblastoma (GBM) Cancer Stem Cells (CSC) cultures

GBM CSC cultures, already validated for CSCs properties and tumorigenicity, were kindly provided by Professor T. Florio's laboratory, University of Genova.

Post-surgical samples were used after patients' informed consent and Institutional Ethical Committee (IEC) approval. All patients underwent surgery at Neurosurgery Department (IRCCS-AOU San Martino-IST) and had not received therapy prior to the intervention. Specimens were histologically classified as GBM grade IV (WHO classification).

CSCs were grown at 37°C with 5% CO_2 in stem cell-permissive medium composed of DMEM and F12-GlutaMAX 1:1, Penicillin/Streptomycin 1% and enriched with B27 supplement 1X, 10ng/ml human bFGF and 20ng/ml human EGF. Cells were grown in suspension as spheroid aggregates (neurospheres) which formation occurred within 1 week of culture. Once a week neurospheres were mechanically dissociated into a single-cell suspension and re-plated in fresh medium to produce secondary neurospheres. In this way is possible to avoid the differentiation of cells in the center of the spheres that are losing contact with the selective medium.

CSCs were also grown in the same medium as monolayer on growth factor-reduced Matrigel coating (BD Biosciences), allowing easier evaluation of viability, immunofluorescence or time lapse microscopy experiments without affecting stem cell features.

3.1.1 G1 synchronization

Monolayers cultures of CSCs have been synchronized in G1 phase of the cell cycle through 36 to 60 hours of starvation in DMEM. Cells are released from the G1 blockage after the switch from DMEM to complete stem-cell permissive medium. For some experiments cells have been released in complete stem-cell permissive medium containing specific compounds (see "reagents")

3.1.2 Transfection

To monitor the oxidative stress, CSCs have been transfected with Cyto-roGFP2-VQ Ad5CMV K-NpA plasmid. This construct expresses the thiol redox-sensitive ratiometric sensor roGFP in the cytosol of mammalian cells.

The cells have been transfected using Lipofectamine LTX and Reagent PLUS (Life Technologies), adapting the Invitrogen “Transfecting Primary Mouse Neural Progenitor Cells using Lipofectamine LTX reagent” protocol .

To transfect 150000 cells, a mix of 6,25 µl of Reagent Plus and 2,5 µg of plasmid in 200 µl of DMEM is prepared. After 15 minutes at room temperature 3,75 µl of Lipofectamine LTX are added to the mix. The mix is left 30 more minutes at room temperature and then added to the CSCs culture which medium have been previously substituted with complete medium without antibiotics. The efficiency of the transfection is checked after 18-24 hours using a fluorescence microscope.

3.2 Umbelical Cord Mesenchimal Stem Cells (uc-MSC) cultures

uc-MSCs were kindly provided by Professor T. Florio’s laboratory, University of Genova. Human umbilical cords were obtained after caesarean section at Obstetrics and Gynaecology Department of International Evangelical Hospital (Genova, Italy), following informed consent and approval by IEC. After vessel removal, cords were treated with collagenase (0.5µg/ml) to expose Wharton jelly and obtain single cells.

Cells were grown at 37°C with 5% CO_2 in MesenPRO RS basal medium+Supplement (Life Technologies) after flow cytometry phenotypical characterization (MSC Phenotyping Kit, Miltenyi Biotec).

3.3 Reagents

Indanyloxyacetic acid 94 (IAA94), (Sigma Aldrich), has been used to inhibit CLIC1 channel activity. Starting concentration: 50 mM in ethanol.

Diphenyleneiodonium chloride (DPI), (Sigma Aldrich), has been used to inhibit NADPH oxidase activity. Starting concentration: 10 mM in DMSO.

5-(N-Ethyl-N-isopropyl)amiloride (EIPA), (Sigma Aldrich), has been used to inhibit NHE1 activity. Starting concentration: 50 mM in DMSO.

N-Formyl-L-methionyl-L-leucyl-L-phenylalanine (FMLP) (Sigma Aldrich), has been used to activate NHE1. Starting concentration: 1 mM in DMSO.

3.4 Electrophysiology

3.4.1 Patch clamp tecnique

The patch clamp technique allows the measurement of the ionic currents passing through ion channels. It was developed by Neher and Sakmann in the late '70s and it has brought great innovations in the fields of physiology and biophysics. In this technique a small heat-polished glass pipette is pressed against the cell membrane where the ion channels are embedded and forms an electrical seal with a resistance of ≈1-10 GΩ[135]. The high resistance of the seal ensures that most of the currents originating in a small patch of membrane flow into the pipette and, from there, into current measurement circuitry. An electrode (a silver wire coated with AgCl), located inside the glass pipette and connected to the circuitry, converts the ionic current into electrical current.

From the cell-attached configuration described above other possible configurations are achievable (Figure 9):

- Inside-out configuration, where the pipette is rapidly withdrawed from the cell-attached configuration without destroying the giga-seal, leaving a cell-free membrane and allowing current recordings in known intracellular solutions.

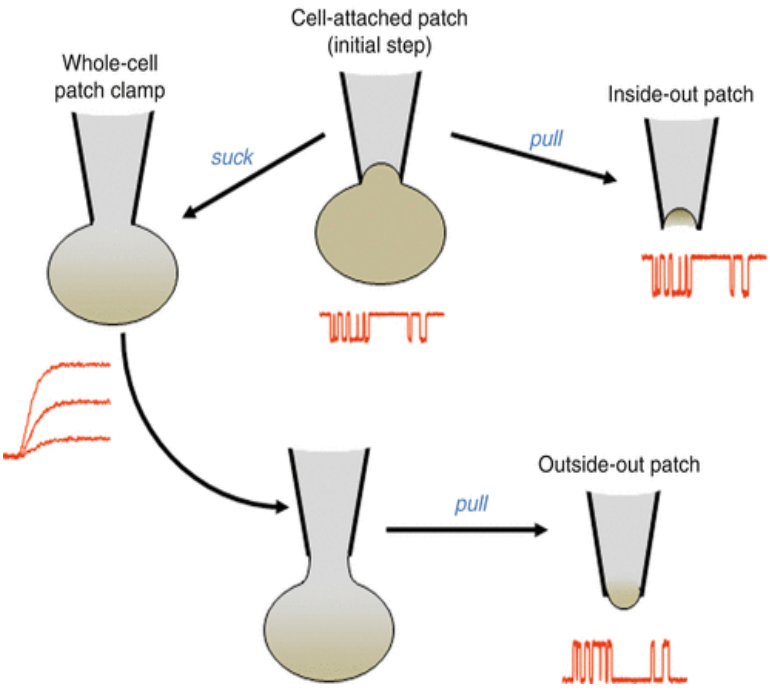

Figure 9: Patch clamp configurations (from Encyclopedia of Biophysics-Patch-Clamp Recording of Single Channel Activity: Acquisition and Analysis Noel Wyn Davies)

- Whole cell configuration, where after giga-seal formation the membrane patch is disrupted providing a direct low resistance access to the cell interior allowing for recordings from the ion channels in the whole cell membrane.

- Outside-out configuration, where the pipette is gently withdrawed from the whole-cell configuration without destroying the giga-seal, leaving a cell-free membrane patch exposing in the bath solution the outer leaflet of the lipid bilayer.

- Perforated patch, where the pipette contains specific antibiotics (gramicidin, amphotericin B, nystatin..) that, once inserted in the plasma membrane of the seal, provide electrical access to the cell interior with the great advantage of preserving the cytoplasm content.

3.4.2 Patch clamp experiments

The patch electrodes (BB150F-8P with filament, Science Products) with a diameter of 1.5 mm, were pulled from hard borosilicate glass on a Brown-Flaming P-87 puller (Sutter Instrument, Novato, CA) and fire-polished to a tip diameter of 1-1.5 µm and an electrical resistance of 3-4 MΩ. The cells were voltage-clamped using an Axopatch 200 B amplifier (Axon Instrument) in the perforated patch configuration. The antibiotic used is Gramicidin

(final concentration in the pipette 5 µg/ml) that forms pore in the membrane permeable only to monovalent cation; in this way the internal chloride concentration of the cells is preserved. Ionic currents were digitized at 5 kHz and filtered at 1 kHz. Clampex 8 was used as the interface acquisition program. The voltage protocol consisted of 800 ms pulses from -40 mV to + 60 mV (20 mV voltage steps). The holding potential was set according to the resting potential of the single cell (between -40 and -80 mV); a 15 ms prepulse of -40 mV is applied before starting the voltage steps, in this way the different recordings are comparable despite the different holding potential.

CLIC1-mediated chloride currents were isolated from the other ionic currents in the cells by perfusing a specific inhibitor (Indanyloxyacetic acid 94; IAA94 100 µM) dissolved in the bath solution.

The solutions used in the patch-clamp experiments of this thesis, referred to the article *'Malignant gliomas display altered pH regulation by NHE1 compared with nontransformed* astrocytes'[131], are the following:

Bath solution (mM): 125 NaCl, 5.5 KCl, 24 HEPES, 1 $MgCl_2$, 0.5 $CaCl_2$, 5 D-glucose, 10 NaOH, pH 7.4.

Pipette solution (mM): 135 KCl, 10 HEPES, 10 NaCl, 1 $MgCl_2$, pH 7,2.

When required for the experiments EIPA 25 µM, DPI 10 µM and/or FMLP 100 nM are added directly in the bath solution starting from 15 minutes before the beginning of the experiments.

3.4.3 Analysis

Offline analysis was performed using Clampfit 10.2 (Molecular Devices) and OriginPro 9.1. CLIC1-mediated current (IAA94-sensitive current, I_{IAA94}) was extimated by analytical subtraction of the residual ionic currents, after the addition of the inhibitor, from the total current (I_{TOT}) of the cell at each membrane potential tested. Current/voltage relationships (I/V curves) were constructed plotting the averaged current density of the last 100 ms of the pulse against the corresponding membrane potential. Current density (pA/pF) results from

the ratio between the ionic current (pA) and the cell capacitance (pF). Error bars are the standard error of the mean in all plots. Statistical analysis were performed comparing the slopes (proportional to the channel conductance) of the I/V curves of the different groups.

3.5 Protein extraction and Western Blot

Cells samples ($2*10^6$ cells each) were collected by scraping directly with lysis buffer (LB; in water: 0.25 M Tris-HCl pH 6,8, 4% SDS, 20% Glycerol) or by centrifugation and resuspension in LB. Complete lysis of the cells was obtained by 10 minutes of incubation in LB at 95°C. Concentration of protein lysates was assessed by BCA assay (Pierce). The same amount of proteins for each sample was loaded onto a 15% SDS-polyacrylamide gel electrophoresis (PAGE) under reducing conditions; before the loading 0.02% Bromophenol Blue and 2.5 % β-mercaptoethanol were added to the samples; resolved proteins were transferred onto Nitrocellulose membranes (Protran) of 0,2 µm pore size into a transfer buffer (glycin 1%, tris-base 0,02 M, methanol 20%) to which is applied a constant voltage.

Membranes were first incubated for 1 hour with 5% BSA in PBS-0,02% Tween to block non-specific binding sites and then 1 hour with primary antibodies diluted in 5% BSA in PBS-0,02% Tween. Antibody binding was assessed by horseradish peroxidase (HRP)-conjugated secondary antibody. Immunoreactive bands were detected with enhanced chemiluminescence reagents (ECL, Pierce).

The antibodies used were the following:

Purified Mouse Anti-Human Retinoblastoma Protein (BD Pharmingen) 1:1000

Mouse monoclonal Anti-tubulin (Sigma) 1:5000

Secondary anti-mouse antibody-HRP conjugated (Sigma) 1:10000

3.6 Immunofluorescence

Indirect immunofluorescence was used to evaluate CLIC1 localization and P27 expression.

CSC's monolayers of 5000 cells for each 12 mm diameter cover glass are washed with PBS Ca^{2+}/Mg^{2+} and fixed with 2% paraformaldehyde in PBS Ca^{2+}/Mg^{2+} for 10 minutes at room temperature. After some washing with PBS Ca^{2+}/Mg^{2+} the samples are permeabilized with Bovine Serum Albumine (BSA) 5%-0,1% Triton X-100 in PBS Ca^{2+}/Mg^{2+} for 4 minutes and non-specific binding sites are blocked through a 30 minutes incubation with BSA 5 % in PBS Ca^{2+}/Mg^{2+}. Cells are washed twice with PBS Ca^{2+}/Mg^{2+} and then incubated with the primary antibody diluted in PBS Ca^{2+}/Mg^{2+} for two hours. After washes with PBS Ca^{2+}/Mg^{2+} the samples are left for one hour in the dark with the secondary antibody diluted in PBS Ca^{2+}/Mg^{2+}, this antibody binds to the primary one and is conjugated with the fluorophore. To visualize cells nuclei the samples were treated 15 minutes with DAPI and then mounted on microscope slides using a glycerol-based mounting agent.

Samples were observed under a confocal microscope Leica TCS SP2 with a Leica HCX PL APO 63X/1.4NA oil immersion objective for figures 10 and 20. To acquire images Leica confocal software was used. Laser lines 405 nm to see DAPI and 488 nm to see green fluorescence were used, the channels were acquired sequentially to avoid crosstalk problems. Samples were observed under a wide field Olympus BX61 upright microscope with a CoolSnap Photometrics camera and 40X oil immersion objective for figure 13. To acquire images the Metamorph software was used. Excitation filters at 405 nm to see DAPI and 488 nm to see green fluorescence were used. Images were analyzed using ImageJ software.

The antibodies used were the following:

Mouse monoclonal anti-human CLIC1 (Santa-Cruz), 1:100

Mouse monoclonal anti-P27 (Santa Cruz) 1:100

Secondary antibody anti-mouse Alexa Fluor 488 (Life Technologies) 1:400

3.7 pH measurement

Intracellular pH (pH_i) is measured using the probe carboxy SNARF-1 AM (carboxy SemiNaphthoRhodaFluor acetoxymethyl ester – Life Technologies), calibrated with high potassium buffers and nigericin, following Chow and Hedley's protocol [136]. The acetoxymethyl (AM) ester form of the dye enters the cells readily and is hydrolyzed by nonspecific cellular esterases to yield the free fluorescent dye. This pH probe is a weak acid with pK_a values close to 7.0. Its protonated and free base forms, both excited at 514 nm, have different emission spectra (580 nm and 640 nm); taking the ratio of the two resulting emissions gives a signal that is proportional to internal pH and independent of cellular dye content. From the equation of a calibration curve, obtained using standards with known pH_i, is possible to extrapolate the intracellular pH of the samples.

Briefly, CSCs are dissociated, centrifuged for 10 minutes at 600 rpm and resuspended in PBS 1X ($1*10^6$cells/1 ml PBS). Each sample contains $5*10^5$ cells in 500 µl of PBS. Carboxy SNARF-1 AM is added to each sample to a final concentration of 5 µM and cells are incubated for 30 minutes at 37°C in the dark. Samples are centrifuged at room temperature, resuspended in 500 µl of the desired solution and incubated for 20 minutes at room temperature in the dark:

Samples: Sodium solution (125 NaCl, 5.5 KCl, 24 HEPES, 1 $MgCl_2$, 0.5 $CaCl_2$, 5 glucose, 10 NaOH, pH 7.4) ± desired treatment

Standards: high potassium buffers (pH 6.8-7.0-7.2-7.4-7.6-7.8) + nigericin (final concentration 2µg/ml)

The standard solutions are obtained mixing 1:1 MES solution (mM: 140 KCl, 1 MgCl2, 2 CaCl2, 5 D-glucosio, 20 MES) and TRIS solution (mM: 140 KCl, 1 MgCl2, 2 CaCl2, 5 D-glucosio, 20 Tris base). Desired pH (6.8-7.0-7.2-7.4-7.6-7.8) is obtained adding an appropriate amount of the alkalinizing (TRIS) or acidifying (MES) solution to the starting solution. Nigericin allows exchange of H^+ for K^+ across their concentration gradients, so that

when external and internal potassium ion concentrations are approximately equal, there is free movement of hydrogen ions and intracellular pH is the same as extracellular pH.

Samples are analyzed by flow cytometry with a FACS Aria (BD Bioscience) to determine the 640/580 fluorescence ratio.

The calibration curve, obtained with the values of the Em_{640}/Em_{580} ratio of the standards, is built using Excel.

3.8 ROS measurement

To measure the redox conditions of the cells, CSCs were transfected with a plasmid carrying the sequence of Cyto-roGPF. Cyto-roGFP plasmid (ligated in the vector VQ Ad5CMV K-NpA) was a gift from Paul Schumacker (Addgene plasmid # 49435). This is a particular Ro-GFP genetically engineered to be express in the cytoplasm of the cells. This redox-sensitive protein emits at 525 nm and has excitation maxima at 400 and 484 nm. In response to changes in redox conditions, RoGFP exhibits reciprocal changes in intensity at the two excitation maxima [137]. Since the probe is ratiometric insensitive to its expression levels.

Cells were transfected with the plasmid as described in the above section, seeded in adhesion on glass-bottom petri-dishes and the treatments added at the specific times (24 hours or 30 minutes before the fluorescence acquisition). Cells expressing the roGFP2 redox sensor were then imaged *in vivo* by an inverted fluorescence microscope Nikon Ti-E (Nikon, JP) with a CFI Plan Apo VC 60X Oil objective. Excitation light was produced by a fluorescent lamp Prior Lumen 200 PRO (Prior Scientific, UK) switching between 470/40 nm and 405/40 nm. Images were collected with a Hamamatsu Dual CCD Camera ORCA-D2 (Hamamatsu, Photonics, JP). The GRX-roGFP2 emissions were collected with a bandpass filter of 505-530 nm for both excitation wavelengths. Exposure time was 100 ms with a 2x2 CCD binning for the 470/40 nm excitation, and 300 ms with a 2x2 CCD binning for the 405/40 nm excitation and images were acquired every 5 sec for 1 minute. Filters and dichroic mirror were

purchased from Chroma (Chroma Technology Corporation, USA). The NIS-Element (Nikon, JP) was used as platform to control microscope, illuminator, camera and post-acquisition analyses. Fluorescence intensities were determined over regions of interest (ROIs) (corresponding to the analyzed cells), background subtracted and used for the ratio (R) (405/488) calculation. The images analyzed using IMAGEJ software.

3.9 Cell cycle analysis

Cell cycle FACS analysis has been performed with a FACS Aria (BD Bioscience). Samples are analyzed at FACS using appropriate filter to visualize the fluorescence emitted by Propidium Iodide (PI) intercalated into the DNA (Em=488 nm; Ex=617 nm) to evaluate the DNA content.

For each sample 2 millions of cells are washed with 500 µl of PBS 1X, centrifuged for 10 minutes at 600 rpm and fixed with 1 ml of cold ethanol 70% in PBS. After at least two hours at 4°C, cells are centrifuged for 3 minutes at 2500 rpm and washed twice with PBS 1X to remove all the ethanol. After the last wash cells are resuspended in 200 µl of staining mix (Propidium Iodide 50 µg/ml, RNAsi 0,2 mg/ml, Triton X-100 0,5% in PBS 1X), incubated 30 minutes at 37°C and directly read at the FACS.

3.10 Viability assays

Mitochondrial function, as index of cell viability, was evaluated by measuring the reduction of 3-(4,5-dimethylthiazol-2-yl)-2,5-diphenyltetrazolium bromide (MTT, Sigma-Aldrich). GBM CSCs were plated in 48-well matrigel-coated plates. The number of cultured cells was adjusted to a density that allowed the cells to grow exponentially for the full duration of the assay (up to 3 days) and thus ranged from 2,500 to 10,000 cells/well. After treatments, cells were incubated in MTT solution (2 mg/ml in PBS) for 2 hours, formazan crystals were

dissolved in DMSO, and absorbance was measured with a spectrophotometer at a 570 nm wavelength.

3.11 Time lapse microscopy

A ScanR Olympus system, with an inverted microscope IX81, a motorized Marzhauser's stage and a Hamamatsu OrcaER camera, equipped with an OKOlab incubator to maintain samples at 37°C and with 5% CO_2 was used to obtain time-lapse videos.

CSCs are plated as monolayers in a 12-wells multiwell, 10000 cells for each well. To acquire the images each well is divided in 15 fields (5X3) and for each field images are taken with an Olympus 10X/0.30NA objective every 15 minutes for 24 hours. Excellence (Olympus) software has been used to acquire images.

To edit the movies it has been employed Image J software

3.12 Data elaboration and statistical analysis

All the data that required statistical validation have been analyzed with the appropriate statistical test.

The current density/voltage relationships of CLIC1 mediated current have been analyzed as following: for each condition every experiment has been plotted and the linear regression for the curve has been extrapolated (all significant, with $R^2 \geq 0.9$). A two-sample T-test, if the condition analyzed were only two, or a one-way ANOVA analysis have been performed on the slopes of every experimental group.

The western blot data are expressed as the intensity of the phosphorilated Rb band normalized on the intensity of the tubulin band. The experiment in figure 1 have been normalized on the value at 0 hours and the experiments in figure 3 on the value at 10 hours. A one sample T-test has been performed to validate the results for figure 3.

The data of the internal pH values have been expressed as the difference between the pH_i of treated cells and the pH_i of untreated cells (ΔpH_i). Thus, an acidification will be indicated by a negative value while an alkalinization by a positive value. The results have been statistically analyzed using a one-sample T-test to confirm the difference from 0 for each group.

4. AIM OF THE THESIS

To propose and validate ion channels as new pharmacological targets it is fundamental a deep analysis of the levels and regulation of their activity during cancer cells proliferation.

This thesis work aimed first of all to validate the specific function of CLIC1, in its transmembrane form, in GBM CSCs proliferation and cell cycle progression, proposing it as a specific target for GBM CSCs.

Once confirmed the role of CLIC1 in the progression from G1 to S phase of the cell cycle, the second aim pursued was to evaluate if the activity of the channel was variable during the progression of G1 phase, in order to assign a specific timing to CLC1 membrane localization during the transition from G1 to S phase.

The last purpose of this work was to study the regulation of CLIC1 channel activity in the progression of G1 phase of GBM CSCs by changes in internal pH and ROS levels. These two factors are known to oscillate during cell cycle progression and to be correlated in their dynamic mechanism.

The general aim of this project is to elucidate the role of CLIC1, pH_i and ROS levels in the cell cycle progression of GBM CSCs. We speculated a feed-forward mechanism, enrolling all these three elements, which sustains the proliferation of these cells. In this scenario CLIC1 is, among the others, the most promising pharmacological target. The functional activity of CLIC1 as an ion channel is indeed specific of pathological conditions, compared to the systems that regulates pH_i and ROS production that are constitutively active even during physiological state. Thus, to hit specifically CLIC1 channel will lower the chance of side effects of the therapy.

5.RESULTS

The experimental work done during my Graduate Studies can be summarized as follow: a systematic series of experiments to understand the mechanisms involving CLIC1 protein that sustain the repetitive cell cycle occurring in human glioblastoma cancer stem cells (CSCs) in culture. To accomplish my objectives I have used several different techniques depending on the different needs. The main achievement of this work is the dissection of the dynamic process underlying the cell cycle progression from G1 to S phase of CSCs. In this scenario CLIC1 protein appears to be an important as well as a peculiar player. Without its contribution CSCs lose the ability to maintain a high mitotic rate.

5.1 Cell cycle progression in GBM CSCs

The functional expression and activity of CLIC1 has been estimated during cell cycle of GBM CSCs to assess the timing of cell cycle progression in these cell cultures.

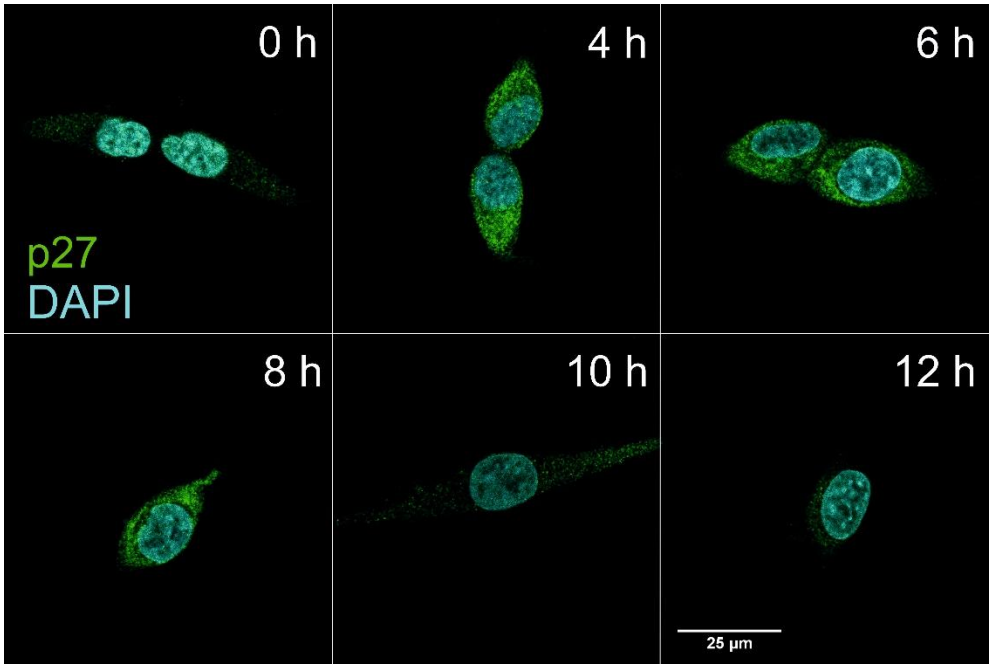

Figure 10: confocal microscope images of p27 expression at different time points from the release from G1 synchronization. The fluorescence associated with the protein clearly decreases at 10 and 12 hours after the release, indicating that the cells begin the transition from G1 to the S phase of the cell cycle.

Indirect immunofluorescence on adherent GBM CSC has been performed to analyze the levels of p27, a CdK inhibitor protein which levels decrease during the progression from G1 to S phase of the cell cycle. The cells have been synchronized in G1 phase, released from the arrest and the samples have been fixed at different times after the release (0, 4, 8, 10,

and 12 hours). At ten hours from the release the fluorescence associated with the levels of p27 expression decreases in intensity (Fig.10). To further confirm the time course of G1 phase progression the levels of phosphorylated Retinoblastoma protein (Rb) have been evaluated through Western Blot analysis. Rb is a protein that, when phosphorylated, becomes inactive and allows cell cycle progression through S phase. The levels of phosphorylated Rb are dependent on p27 decrease.

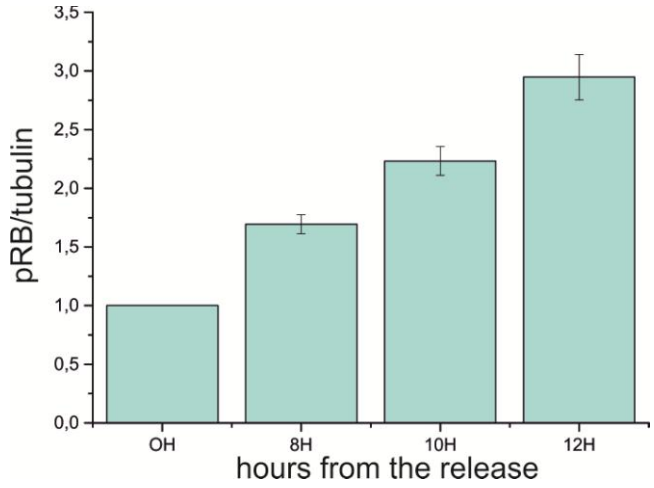

Figure 11: levels of phosphorilated Rb (pRb) protein, normalized on tubulin, at different time points from the release from G1 synchronization. According with the data of p27 levels at 10 and 12 hours from the release pRb levels markedly increase.

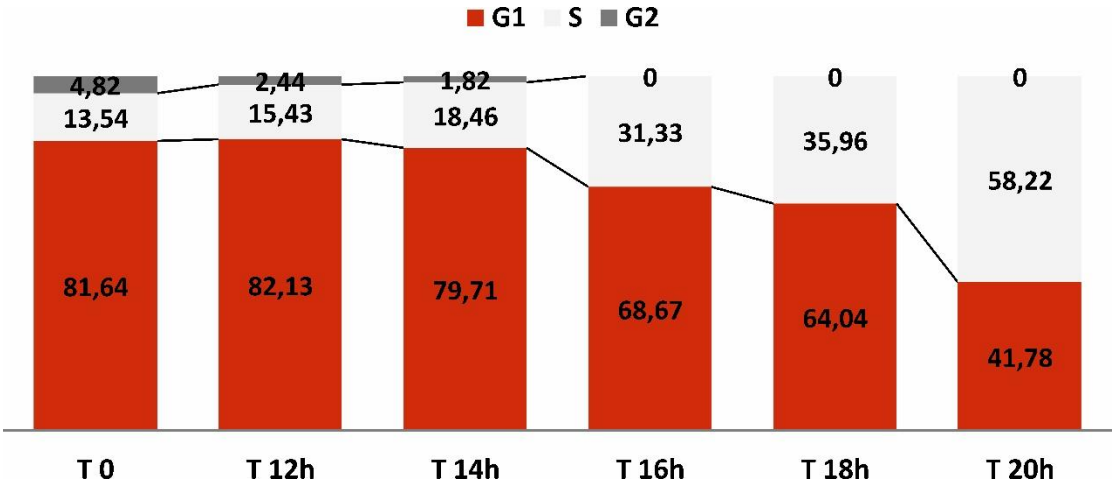

Figure 12: FACS analysis of cell cycle distribution (in%) of CSCs at different hours from the release from G1 synchronization. After 16 hours more than 30% f the cells analyzed were already in S phase, this percentage reached almost 60% after 20 hours.

The quantification of the levels of phospo-Rb normalized with tubulin levels (n=3) showed a marked increase from 8 to 10 and then 12 hours from the release from G1 arrest (Fig.11).

These results were in accordance with the timing delineated by the previous experiment on p27 expression.

To evaluate the time span of the transition to the S phase, we run a FACS analysis after PI staining at different time points after the release from G1 arrest of the cells. The times chosen were 0, 12, 14, 16, 18, 20 hours. At 16 hours after the release almost 30% of the cells were in the S phase (Fig.12).

5.2 Effect of CLIC1 inhibition on CSCs cell cycle progression

Once defined the timing of the transition of CSCs from G1 to S phase, we wanted to confirm the effect of CLIC1 inhibition on the cell cycle and on proliferation of these cells.

We performed immunofluorescence analysis of p27 levels at 12 hours from the release of cells treated or not treated with 100 µM IAA94, the specific inhibitor of CLIC1 channel activity. The samples treated with IAA94 showed higher levels of p27 expression after 12 hours from the release (Fig.13).

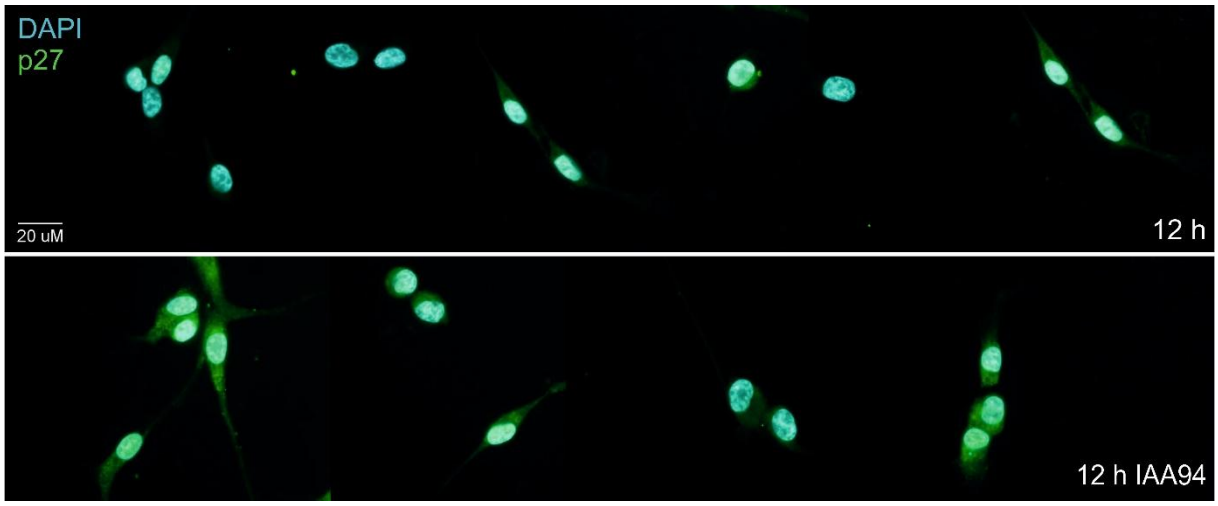

Figure 13: wide-field microscope images of p27 protein expression at 12 hours from the release from G1 synchronization in CSCs released in medium with or without IAA94 100 µM. The cells released in the medium containing the inhibitor at 12 hours showed still high levels of p27 protein.

To further confirm this evidence, we performed a western blot analysis of phosphorilated Rb levels on CSC treated or not treated with IAA94 at 10 hours from the release from G1 arrest. The samples treated with IAA94 showed a significant decrease in the levels of phospo-Rb compared to the controls (Fig.14).

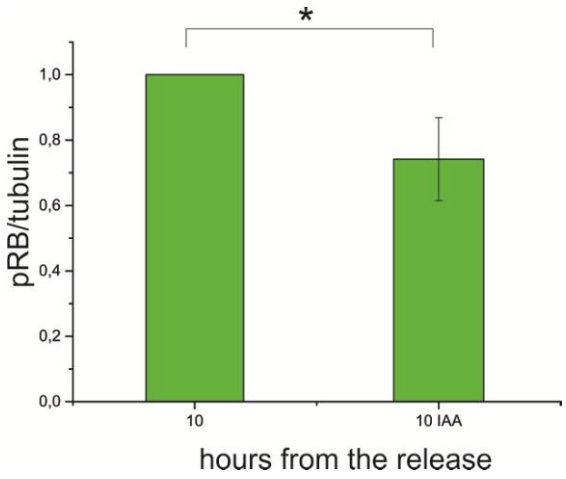

Figure 14: levels of phosphorilated Rb (pRb) protein, normalized on tubulin, at 10 hours from the release from G1 synchronization in medium with or without IAA94 100 µM. The cells released in IAA94 showed a significant decrease in the phosphorilation of Rb (n=3, One sample T-test, p<0,05)

To observe the effect of CLIC1 inhibition on the percentage of cells progressed to S phase, FACS analysis has been carried out after PI staining of CSCs treated or not treated with 100 µM IAA94 after the release from G1 arrest. The time points chosen were 0, 14, 16, 20 hours.. At 16 and 20 hours from the release a higher percentage of the cells treated with IAA94 was still in G1 phase compared to control condition (Fig.15).

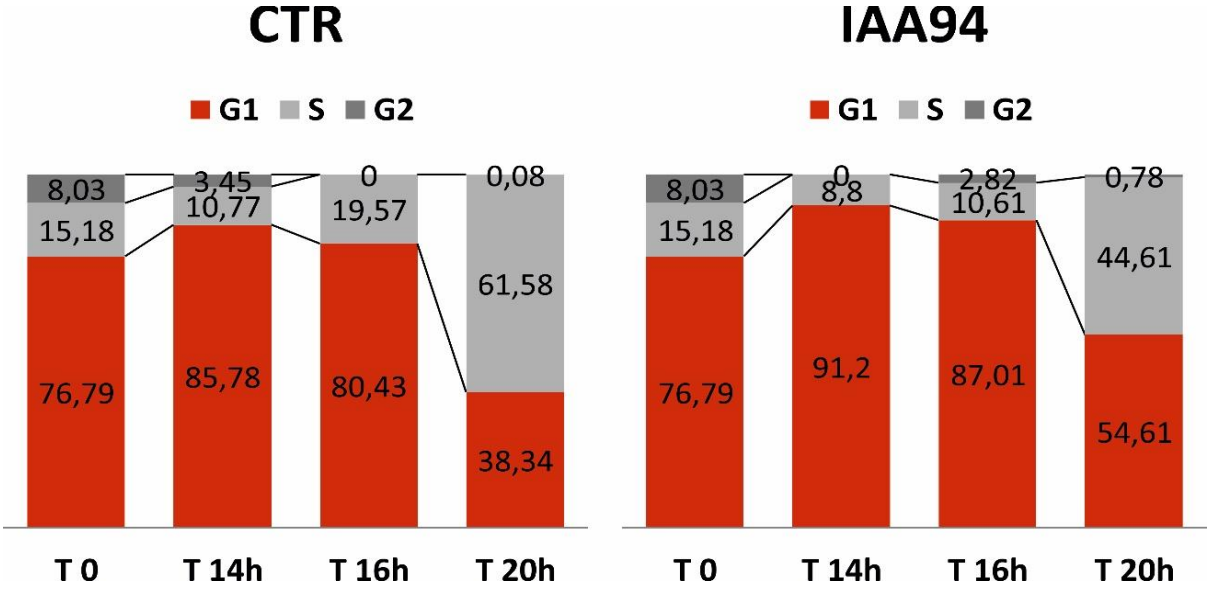

Figure 15: FACS analysis of cell cycle distribution (in%) of CSCs at different hours from the release from G1 synchronization in medium with or without IAA94 100 µM. After both 16 and 20 hours from the release the percentage of cells still in G1 phase was higher in the samples treated with IAA94.

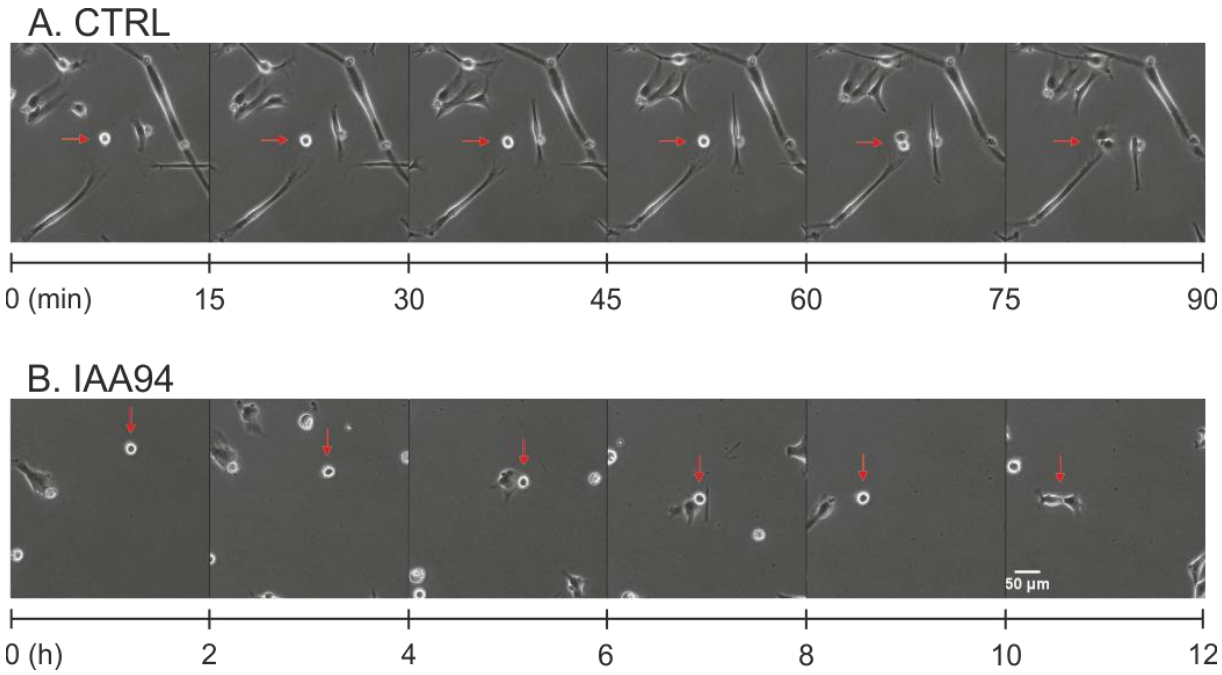

Figure 16: Freeze frames of the videos 1 (CTRL) and 2 (IAA94) attached showing typical dividing times observed for the cells treated (B) or not treated (A) with 100 µM IAA94 in randomly growth conditions. The treatment with the inhibitor lead to a markedly slower dividing time

Video microscopy is very useful to observe, in live condition, the effect of a particular cell treatment. In our case we recorded for 24 hours the behavior of GBM CSCs in the absence

or in the presence of the CLIC1 inhibitor IAA94. Particular attention was devoted to the cell division time. CSCs treated with IAA94 showed a lower rate of dividing cells and a longer dividing time (Videos 1 and 2, Fig.16).

5.3 CLIC1 channel specificity in the proliferation CSCs

It is important to evaluate the specificity of CLIC1 channel activity in the proliferation of CSC compared to other non-tumorigenic stem cells. For this purpose we performed MTT-viability assays on CSCs and umbilical cord mesenchymal stem cells (MSC) treated with different doses of IAA94 (n=3). CSCs viability was almost 50% when treated with IAA94 30 µM (IC50: 32µM). On the contrary MSC weren't affected by the treatment even at 100 µM suggesting that CLIC1 channel inhibition do not have any effect on the proliferation of these cells (Fig.17).

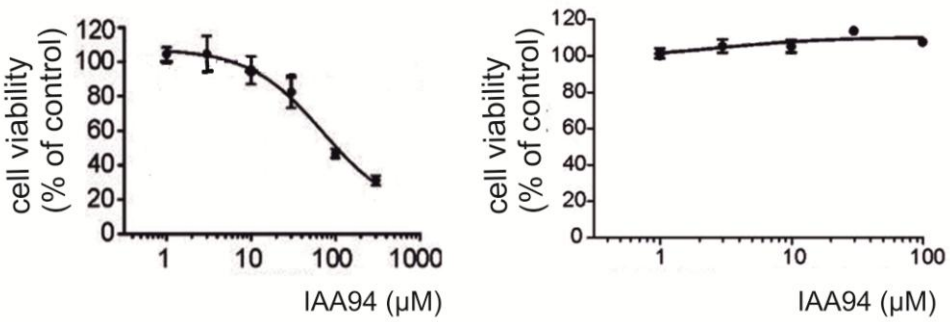

Figure 17: Viability of CSCs and MSCs treated for 24 hours with different doses of IAA94 (n=3). For CSCs the EC_{50} of IAA94 was 32 µM while MSCs were not affected by the treatment even when the concentration reached 100 µM. On CSCs 30 µM IAA94 (One way ANOVA, Dunnet test p<0,01) and 100 µM (One way ANOVA, Dunnet test p<0,001) significantly decrease the growth of the cells compared to control conditions.

FACS analysis of cell cycle distribution on MSCs treated for 72 hours with IAA94 100 µM revealed the absence of effect of CLIC1 inhibition (Fig.18).

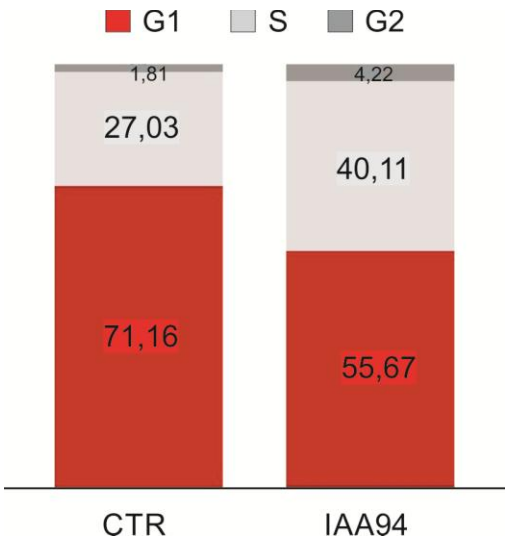

Figure 18 FACS analysis of cell cycle distribution (in %) of MSCs treated (right) or not treated (left) for 72 hours with IAA94 100 µM. After the treatment there isn't an increase in cells in G1 phase as observed for CSCs (Fig.8)

Thus, to check if this missed effect of IAA94 on MSCs proliferation was associated with a lower amplitude of CLIC1 mediated chloride current compared to CSCs, we used an electrophysiological approach. Figure 19 reports patch-clamp experiments in the whole-cell perforated-patch configuration. In all the experiments carried out in our investigations CLIC1 mediated current has been isolated by a mathematical subtraction using current recordings from control versus treated experiments (Fig.19). Steady state currents amplitude at the different membrane potential has been used to build a current/voltage relation showed in Figure 20.

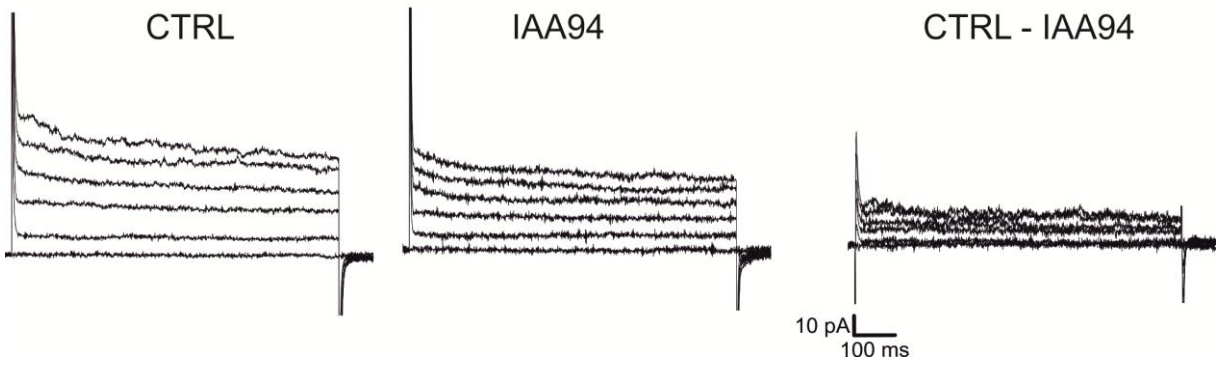

Figure 19: representative current traces recorded from patch clamp experiments in whole cell perforated patch configuration, the protocol provides 6 steps of potential from -40 mV to +60 mV. On the left is depicted the current of the entire cell in control conditions, at the beginning of the experiment. In the trace in the middle there is the residual current after the inhibition of CLIC1 through the perfusion with IAA94 100 µM. The last current trace represents the current mediated by CLIC1 obtained from the subtraction of the current after IAA94 (middle) to the current at the beginning of the experiment (left).

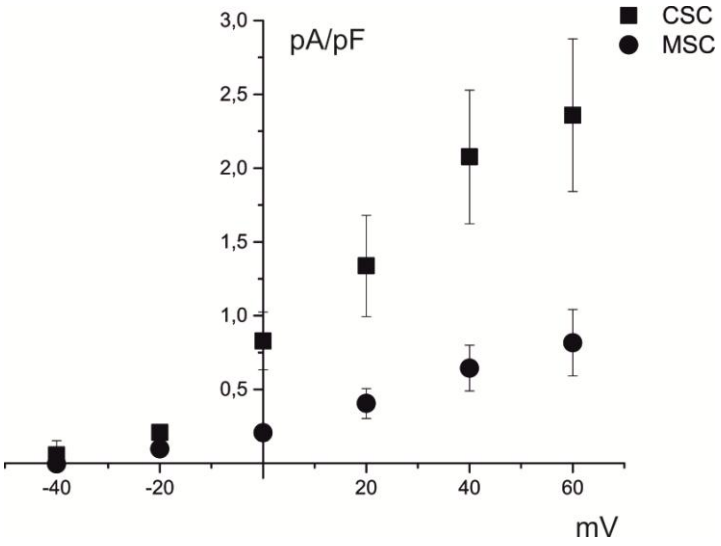

Figure20: current density/voltage relationships of CLIC1 mediated chloride current in MSCs (n=5) and CSCs (n=8). CSCs showed a significantly higher (Two sample T-test, p<0.05) current compared to MSCs.

The experiments performed showed that the medium CLIC1-mediated current density recorded in MSC is significantly lower than in CSCs.

5.4 CLC1 functional expression during cell cycle progression

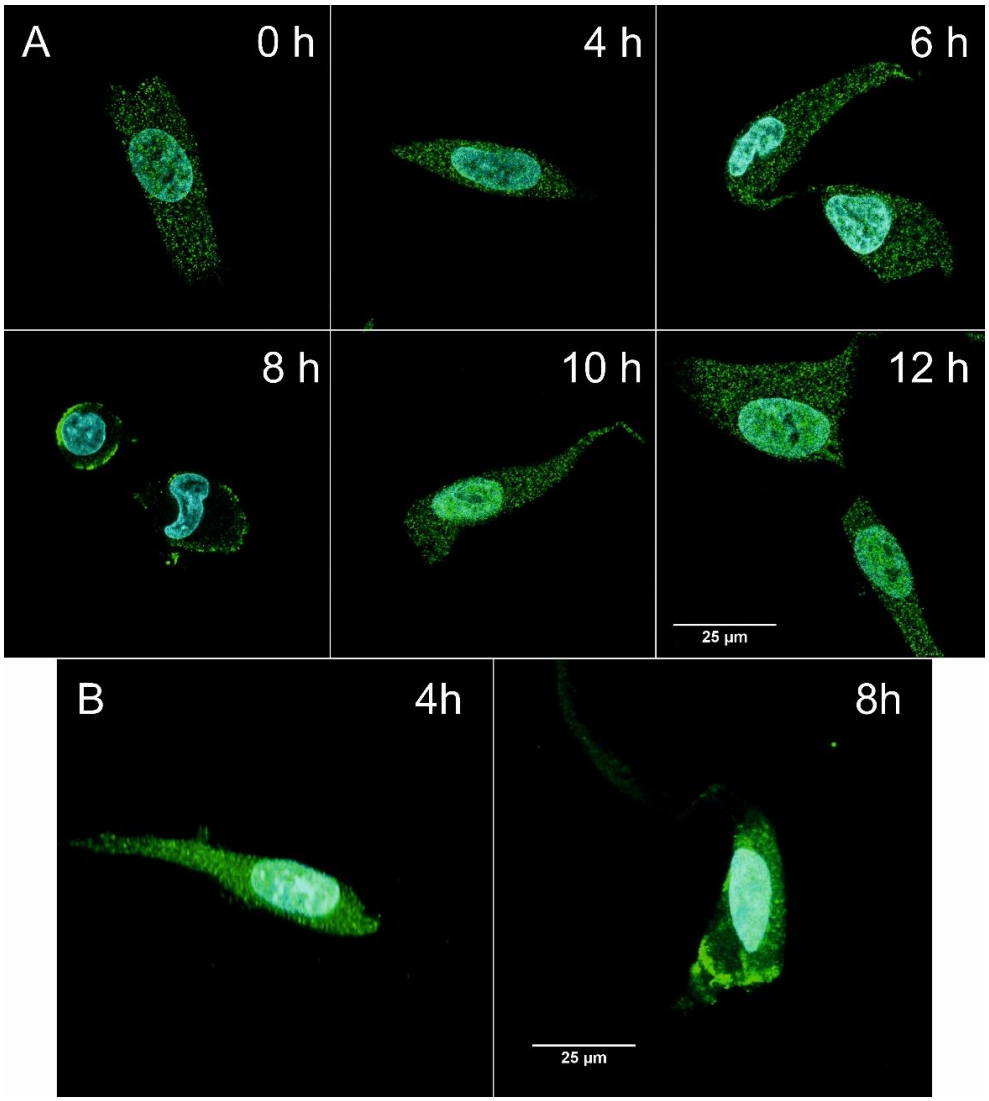

Figure 21: A. confocal microscope images of immunolocalization of CLIC1 in GBM CSCs at different time points from the release from G1 arrest. At 8 hours from the release there is a marked localization of the protein at membrane level. B. The freeze frames of the 3D reconstruction videos (Video 4 and 6) of one cell at 4 hours (left) and one cell at 8 hours (right) from the release highlight the accumulation of CLIC1 in the plasma membrane at 8 hours

Since the blockage of CLIC1 channel activity leads to an accumulation of CSCs in G1 phase, we verified whether CLIC1 membrane localization changes during G1 phase progression. To do this we performed an indirect immunolocalization for the protein on GBM CSCs fixed at different hours from the release from G1 arrest. In Figure 21 it is clear that the protein levels is high during all the time points but after 8 hours from the release there is a clear

accumulation of CLIC1 at the membrane level. The Z-stuck and the 3D reconstruction of the cell at this time point confirm the data (Fig.21 B, Videos 3-4 and 5-6).

To confirm that this membrane localization was associated with the channel activity we repeated perforated patch clamp electrophysiology experiments to monitor CLIC1 mediated chloride current at different hours from the release. Figure 22 compares IAA94 sensitive current amplitude obtained from synchronized cells at different time points from the release with data from randomly cycling CSCs. The increase of the current is evident between 4 and 10 hours with a high value at 8 hours after the cells release. This in accordance with previous experiments demonstrating that CSCs are moving from G1 to S phase in the interval between 4 and 10 while at 18 hours cells have already progressed to S phase.

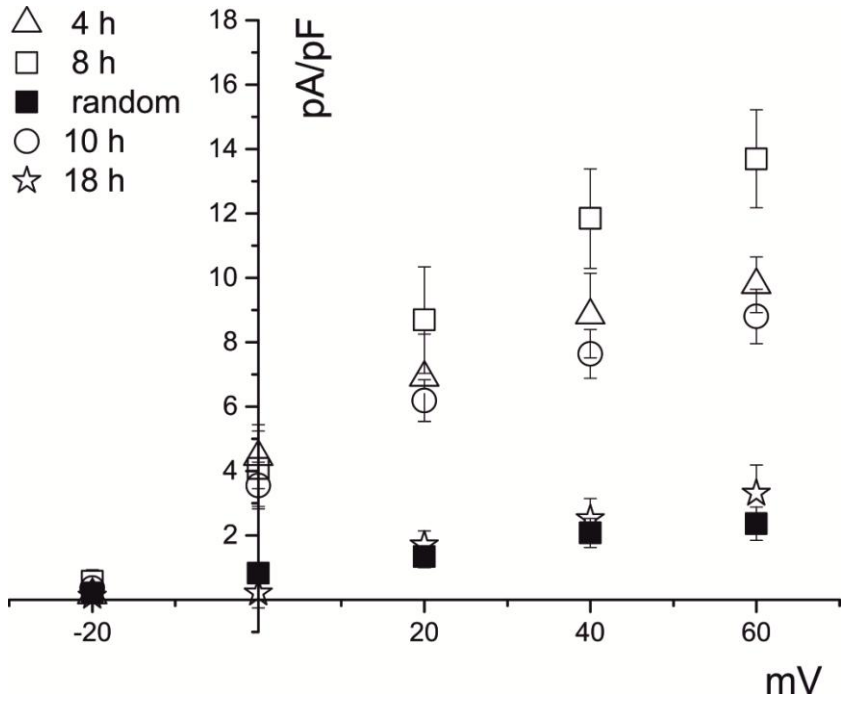

Figure 22: current density/voltages relationships of CSCs at different times from the release from G1 synchronization (4 hours n=5, 8h n=7, 10h n=5, 18h n=7) and randomly cycling (n=8). At 8 hours the increase in CLIC1 mediated current is significant compared to all the other conditions (One Way ANOVA, p<0.001 Tukey test vs randomly cycling cells and 18 hours, p<0.01 Tukey test vs 10 hours, p<0.01 Fisher test vs 4 hours). At 4 and 10 hours the increase is still significant compared to randomly cycling cells and cells at 18 hours from the release (One Way ANOVA, p< 0.001 compared with randomly cycling cells and 18 hours). Cells at 18 hours from the release showed a current superimposable to the current of randomly cycling cells.

From this experiments it is possible to affirm that CLIC1 functional expression in the plasma membrane is maximum after 8 hours from CSCs release from synchronization. These data

are parallel with the result obtain with FACS analysis supporting the idea that CLIC1 chloride current is important for the cell cycle progression from G1 to S phase. In addition, current recordings at 18 hours showing a decrease of the current at the levels of control cells, strongly support the idea of a transient behavior of the IAA94 sensitive current.

5.5 pH levels during cell cycle progression

It is known that in artificial systems pH changes could influence CLIC1 membrane insertion [4]. Thus we wanted to verify whether pH oscillations, occurred during cell cycle progression of GBM CSCs, could influence CLIC1 activity. Using the SNARF1-AM dye we obtained a measure of the internal pH (pH_i) with a cytofluorimetric analysis of CSCs from 3 to 12 hours after the release from G1 arrest (Fig.23). It is evident that between 8 and 10 hours from the release there is a peak in pH_i levels. This time interval corresponds to the time at which CLIC1 membrane current increases (Fig. 22) supporting the idea of an interplay between pH_i and CLIC1 functional expression as an ion channel in the plasma membrane.

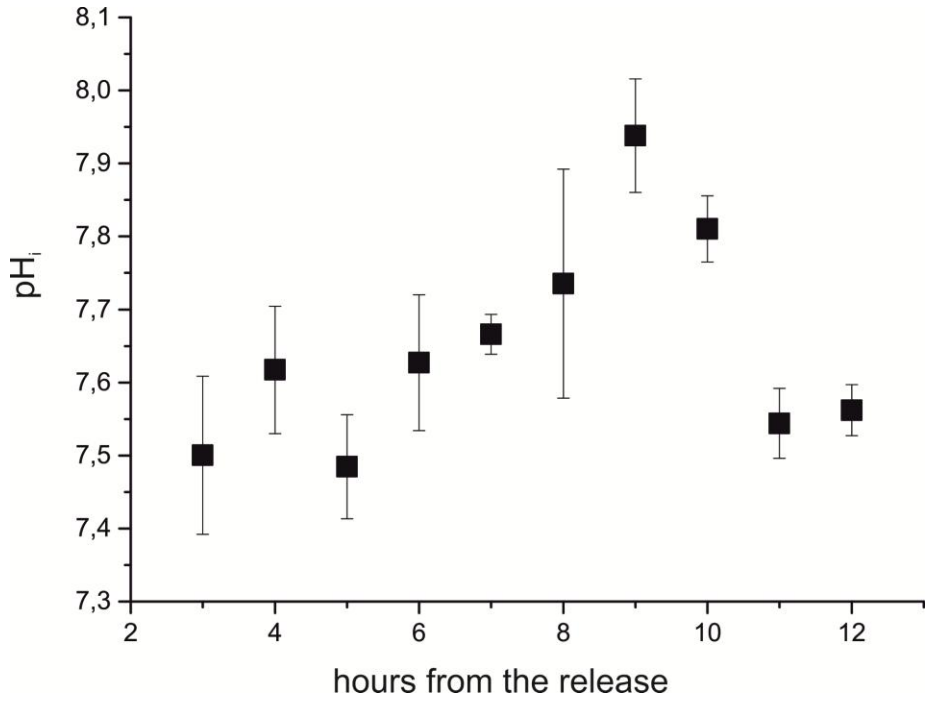

Figure 23: internal pH of GBM CSCs during G1 phase progression (from 3 to 12 hours after the release from G1 synchronization, n=3). Between 8 and 10 hours a peak in the pH_i levels has been recorded.

5.6 pH regulation of CLIC1 channel activity

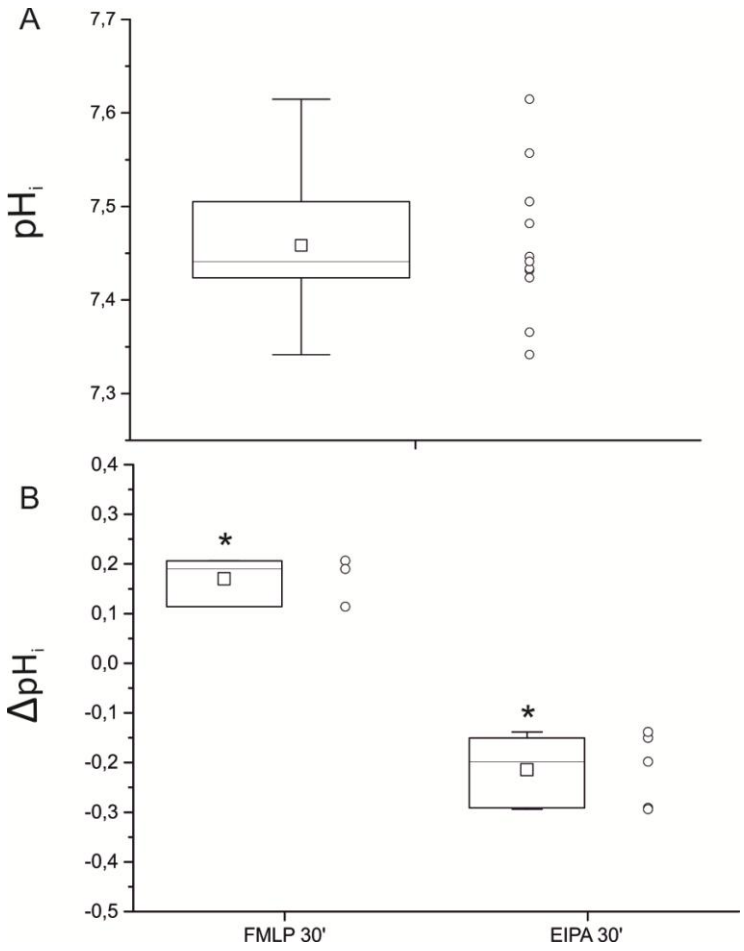

Figure 24: A. internal pH values for GBM CSCs, the mean of 11 measuements was 7.46. B. treatment with FMLP 100 nM (NHE1 activator) lead to a significant increase of pH_i of 0.17 units (n=3, One sample T-test p<0.05); treatment with EIPA 25 µM (NHE1 inhibitor) lead to a significant decrease of pH_i of -0.19 units (n=4, One sample T-test p<0.05)

It is known that glioblastoma cell lines have a higher internal pH compared to non-transformed astrocytes and that pH_i regulation relies mostly on the Na^+/H^+ exchanger NHE1 [131]. Using the SNARF1-AM dye we measured pH_i of GBM CSCs culture randomly cycling. This procedure has been instrumental to study, in the short time range, the intimate relation between the pH_i and CLIC1 protein functional expression. The modulation of the cytosol hydrogen ions content can be achieved using two different compounds with opposite action. One inhibitor (EIPA, 25 µM) and one activator (FMLP, 100 nM) of the NHE1 have been evaluated.

The average pH_i of CSCs was 7.46; EIPA treatment leads to a significant decrease in pH_i levels of about -0.19 pH unit. On the contrary FMLP treatment leads to a significant increase of internal pH of about 0.17 pH units (Fig.24).

Since previously we observed a pH increase in the progression of G1 phase of CSCs cell cycle (Fig. 23), we checked if an induced alkalinization, using FMLP, could increase CLIC1 membrane localization and channel activity. Figure 25 shows immunolocalization for CLIC1 on CSCs treated for 30 minutes with 100 nM FMLP. The same treated cells were under electrophysiological investigation (Fig.26) to evaluate CLIC1 current density. Both experimental procedures confirmed that CLIC1 membrane localization increases and CLIC1 mediated current is significantly augmented with cytosol alkalinization.

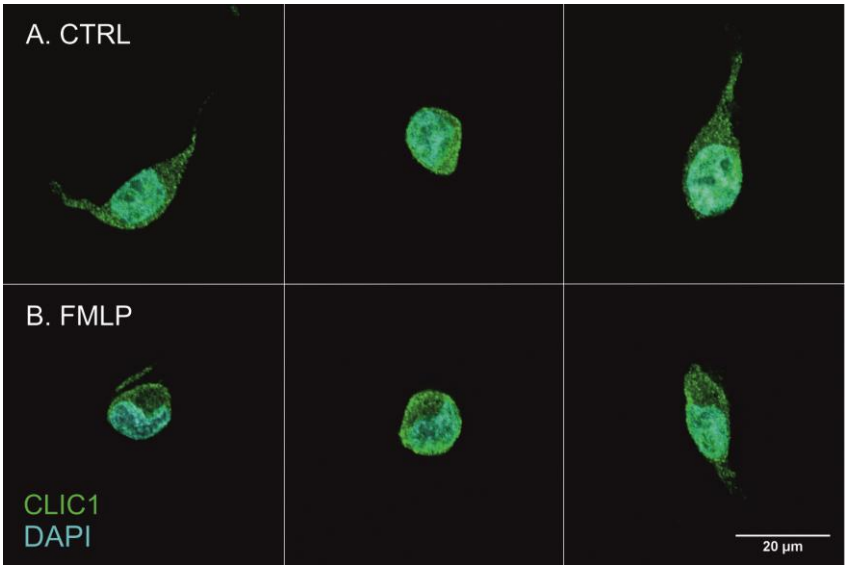

Figure 25: confocal microscope images of immunolocalization of CLIC1 protein in CSCs treated or not treated with 100 nM FMLP for 30 minutes. The increased in pH_i due to FMLP treatment leaded to a higher accumulation of the protein at the membrane level.

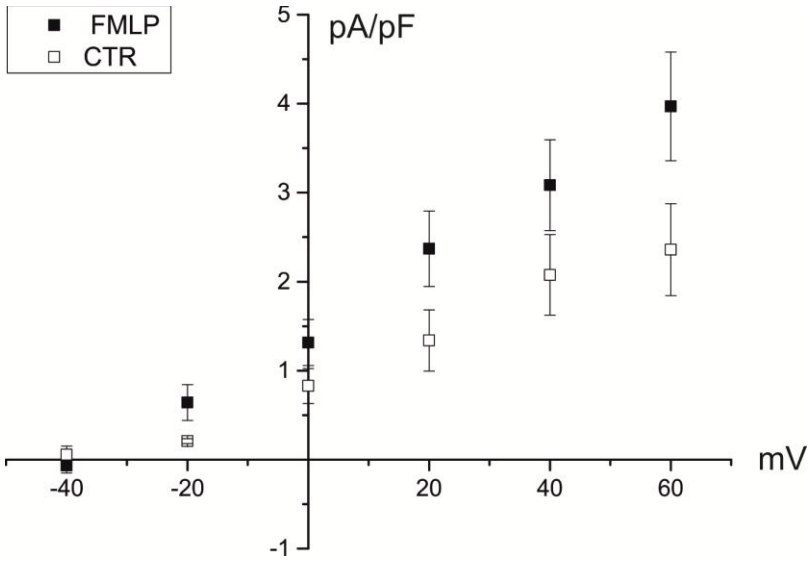

Figure 26: current density/voltage relationships for CLIC1 mediated current in CSCs pretreated (n=10) or not (n=8) with 100 nM FMLP. The increased in pH_i due to FMLP treatment leaded to a significant increase (Two saple T-test, p<0,05) in the current that passes through CLIC1

Since these experiments showed that higher pH_i is able to increase CLIC1 channel activity, we decided to verify if preventing the increase in the internal pH during G1 phase progression could counteract the increase of CLIC1 mediated current observed at 4 and 8 hours from the release from G1 arrest. We went back to perform electrophysiology experiments in perforated patch on GBM CSCs released from G1 arrest in which we added in the medium 25 µM EIPA. Already at 4 hours but most at 8 hours the treatment with EIPA and so the impossibility to increase pH_i results associated with a significant decrease in CLIC1 mediated current (Fig.27).

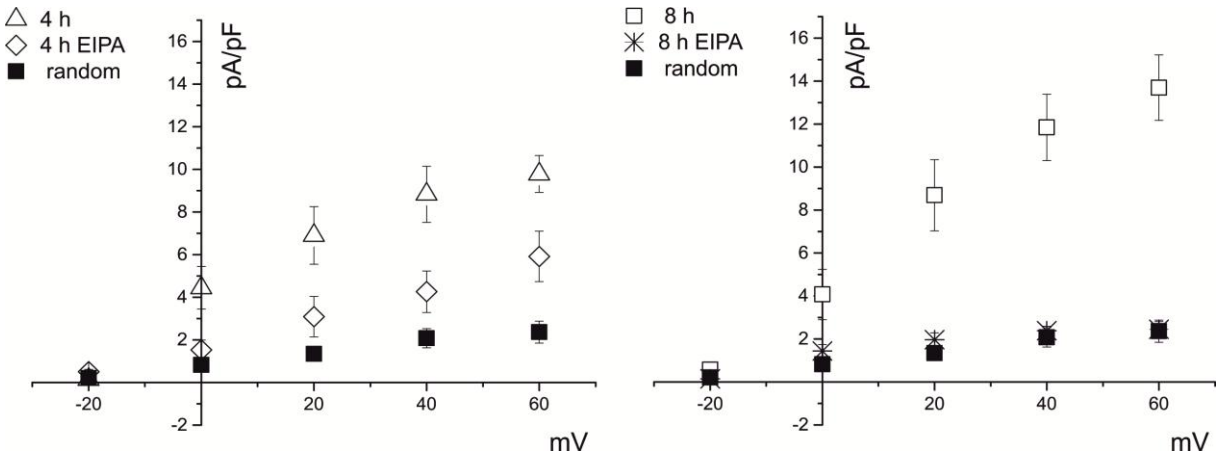

Figure 27: current density/voltage relationships of CLIC1 current in CSCs released from G1 arrest in medium with or without EIPA 25 µM to prevent the increase of pH_i . Already at 4 hours from the release (left) (n=5, One way ANOVA, Fisher test p<0,05) but more clearly at 8 hours(right) (n=4, One way ANOVA, Tukey test p<0,001) the treatment with EIPA caused a significant decrease in the current compared to the corresponding untreated conditions.

5.7 Effect of CLIC1 current inhibition on pH_i

It is known that in activated microglia not only NADPH oxidase activity increases CLIC1 mediated current but also that this chloride current sustains NADPH ROS production [45]. Therefore we verified if, with a similar feed-forward mechanism, the inhibition of CLIC1 channel functional activity could have some effects on internal pH regulation. Thus we evaluated the internal pH using SNARF1-AM after treatment with IAA94 for 30 minutes and for 24 hours or after the co-treatment with IAA94 and EIPA for 30 minutes or IAA94 and FMLP for 24 hours (Fig.28).

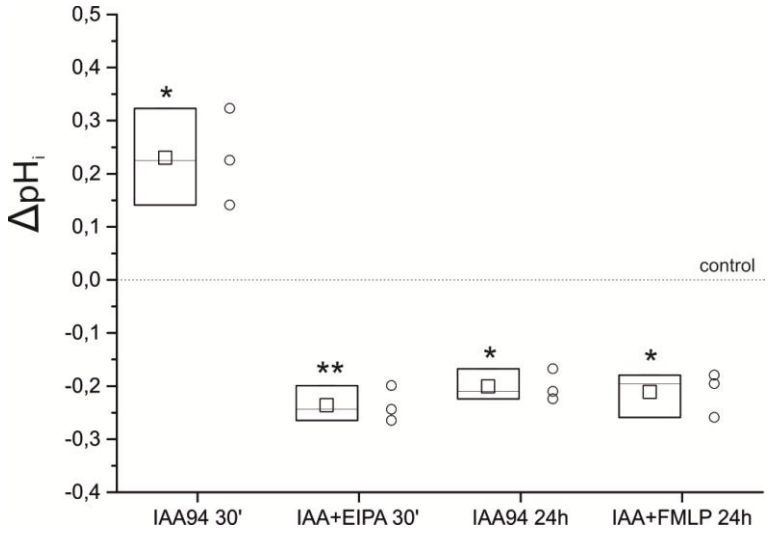

Figure 28: pH_i measurement of CSCs treated with IAA94 100 µM. An acute 30' treatment significantly alkalinized the cells (+ 0.23 units, n=3, One sample T-test p<0.05) , the alkalinization was counteracted by the co-treatment with EIPA 25 µM that brings the pH_i to a more significant acidic level compared with the control (n=3, One sample T-test p<0.01). A chronic 24 h treatment significantly acidified the cells (-0.17 units, n=3, One sample T-test p<0.05) and the effect was not counteracted by the co-treatment with FMLP 100 nM (n=3).

These experiments show that an acute IAA94 treatment leads to a significant increase in pH_i of average 0.23 pH units that is completely counteracted by the co-treatment with EIPA, while a chronic CLIC1 inhibition leads to a significant acidification of average -0.17 units that is not recovered by the co-treatment with FMLP. Starting from the effect of IAA94 observed on pH_i, we performed preliminary trials with CSCs released from G1 synchronization in the medium containing 100 µM IAA94. Figure 29 shows the three most interesting time points, 8,9 and 10 hours from the release. The treatment with the inhibitor decreases the pH_i at all

the time points analyzed obstructing the increase of pH_i observed between 8 and 10 hours from the release showed in the previous section (Fig.22).

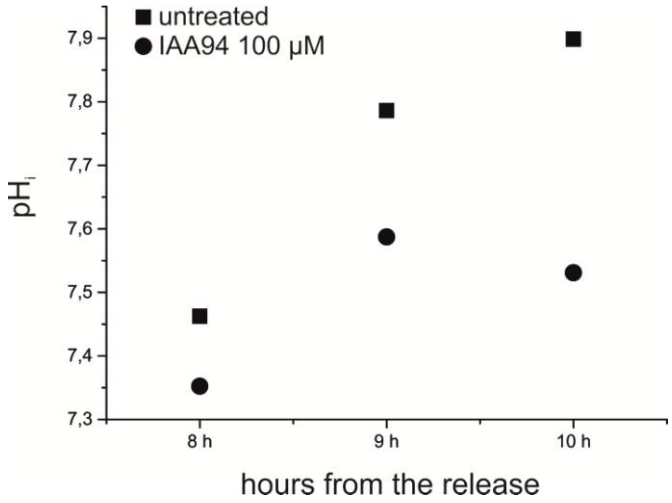

Figure 29: pH_i of CSCs at 8,9 and 10 hours from the release from G1 synchronization in medium with or without IAA94 100 µM. When cells are treated with the inhibitor the increase in pH_i is prevented.

5.8 ROS regulation of CLIC1 channel activity

Since is known that an increased NADPH oxidase (NOX) activity increases CLIC1 mediated current [45] and that an increase in ROS levels is also fundamental to progress from G1 to S phase of the cell cycle [138], we checked if the increase of CLIC1 mediate current observed at 4 and 8 hours from the release from G1 arrest was sensitive to NOX inhibition and so to ROS levels decrease.

Thus, we performed perforated-patch electrophysiology experiments on GBM CSCs released from G1 arrest in a medium containing 10 µM DPI, a NOX inhibitor. Both at 4 and 8 hours from the release the CSCs released in the medium containing DPI showed a significant decrease in CLIC1-mediated current density compared to untreated cells at the same time points (Fig. 30).

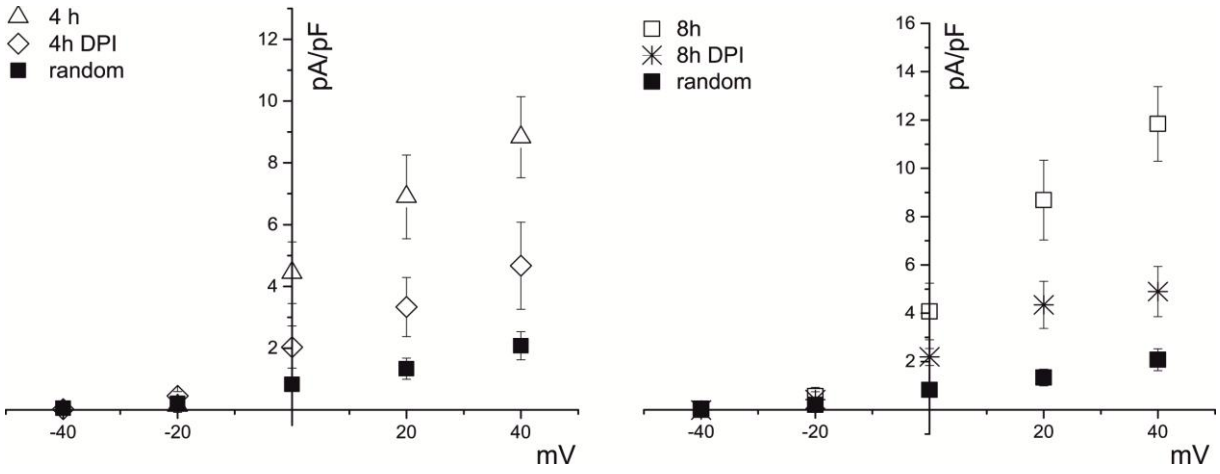

Figure 30: current density/voltage relationships of CLIC1 current in CSCs released from G1 arrest in medium with or without DPI 10 µM to prevent the increase ROS levels . Both at 4 (n=6, One way ANOVA, Tukey test p<0,05) and 8 hours (n=5, One way ANOVA, Tukey test p<0,05) the treatment with DPI caused a significant decrease in the current compared to untreated conditions.

5.9 Effect of NADPH oxidase inhibition on pH_i

It is known that the internal pH and the ROS levels of the cells, especially related to NOX activity could influence each other [139, 140].

To evaluate the effect of NADPH oxidase inhibition on the internal pH we measure hydrogen ion concentration using SNARF1-AM after the treatment with DPI 10 µM for 30 minutes or 24 hours. In Figure 31 the experiment showed that both the treatments significantly decrease pH_i, even if the acute treatment lead to a more evident result. In both cases the co-treatment with DPI 10 µM and FMLP 100 nM counteract this effect.

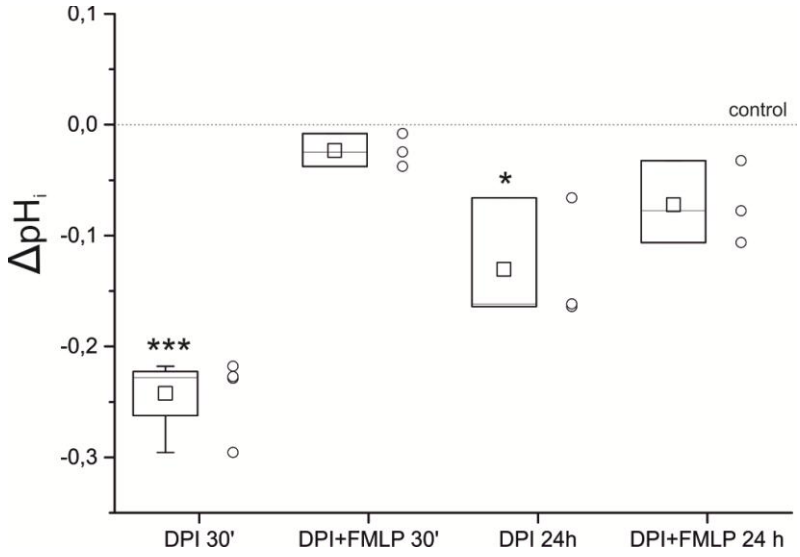

Figure 31: pH_i measurement of CSCs treated with DPI 10 µM. An acute30' treatment leaded to a strongly significant acidification (-0.24 units, One sample T-test p<0.001). A chronic 24 h treatment still significantly acidified the cells (-0.13 units, One sample T-test p<0.05). Both the effect were counteracted by the co-treatment with FMLP 100 nM (n=3 for both) that brings the pH_i to levels no more significantly different from the control.

5.10 Recovery of CLIC1 activity after pH increase

After we observed an effect on pH_i when NOX activity was inhibited with DPI, we verified if the inhibition in CLIC1 current increase at 4 and 8 hours from the release from G1 arrest due to the DPI treatment could be, at least partially recovered by an induced pH_i increase. Thus, the cells have been released in a medium containing both FMLP 100 nM and DPI 10 µM to increase the pH simultaneously with NOX inhibition (Fig.32). The experiments showed that the co-treatment with the two compounds leads to a partial, but significant recovery of the decrease in CLIC1-mediate current density both at 4 (n=7) and 8 (n=12) hours from the release. Infact, the current density/voltage relationships of CSCs released in DPI plus FMLP at 4 hours and 8 hours were no more significantly different from the corresponding untreated conditions.

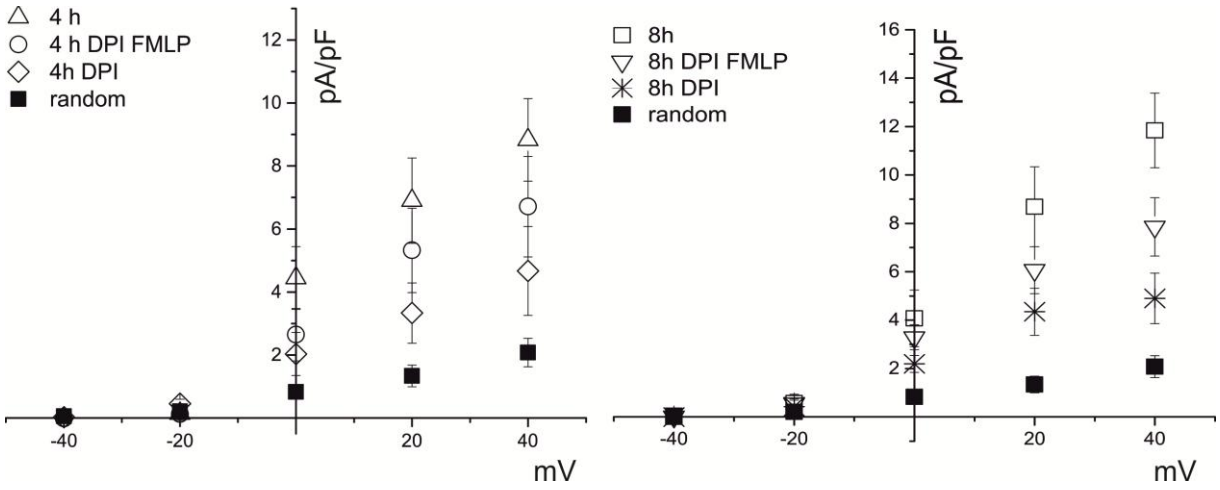

Figure 32: current/voltage relationships of CLIC1 current in CSCs released from G1 arrest in medium with or without DPI 10 µM plus FMLP 100 nM to increase pH_i while decreasing ROS production. Both at 4 (n=7) and 8 hours (n=12) the simultaneous treatment with the two compounds leaded to the loss of significant difference in the amplitude of the current compared to untreated conditions. On the other hand, the currents of the cells treated with both compounds both at 4 and 8 hours returned to be significantly different from the randomly growing cells (4 hours: One way ANOVA, Tukey test, p<0,05; 8 hours: One way ANOVA, Tukey test, p<0,01)

5.11 Effect of CLIC1 current inhibition on ROS levels

To verify if, like in activated microglia [45], also in CSCs a feed-forward mechanism between CLIC1 current and NOX activity is present, we measured the oxidative levels of the cells. To do this it has been exploited the construct cytoRo-GFP that, as described in the methods section, is excited both at 405 and 488 nm and in response to changes in redox conditions exhibits reciprocal changes in intensity at the two excitation maxima. Since in the literature there are no data about the use of this probes in primary cell cultures, the optimal conditions for the transfection of the cells with the plasmid and for the performance of the experiments have been defined after some trials.

The first experiments performed have been carried out on CSCs transfected with the plasmid and treated with IAA94 100 µM for 30 minutes and 24 hours.

Unfortunately the samples treated for 30 minutes in the first two trials gave not congruent results. On the other hand, the cells treated for 24 hours with the inhibitor showed a decrease in the oxidative status compared with the control (n=2) (Fig.33). This is a promising

result that will be confirmed with more trials in which the experimental conditions will be even more optimized.

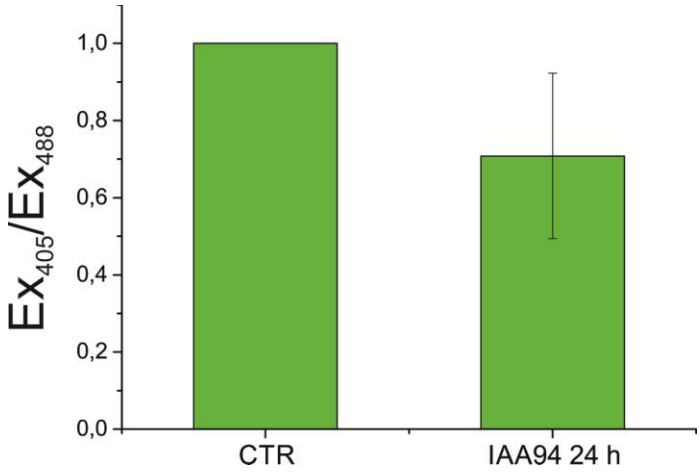

Figure 33: ROS levels evaluation in CSCs treated for 24 hours with IAA94 100 µM. The results are normalized on the level of the ratio Ex_{405}/Ex_{488} of the cells in control conditions. The treatment with IAA94 lead to a decrease (n=20) in the oxidative levels of the cells.

6. DISCUSSION

Allostasis, in the living organisms, is defined as the process of achieving a new state of transient stability through physiological or behavioral changes. Allostasis is essential in order to maintain internal viability during changing conditions. When allostasis become chronic, due to constant stress exposure or due to the failure of the cell systems to restore the homeostatic conditions, it causes a situation of allostatic overload that might lead to pathological conditions. The concept of allostasis envisions a cascade of causes and effects that begins with primary stress, leads to primary modulation and then to secondary and maybe tertiary outcomes, until a new equilibrium arises [141, 142]. Allostasis and allostatic overload can be applied to biological entities from ensemble of organs, functional systems, tissues and also to single cells.

The general hypothesis sustaining this thesis work concerns the concept that during gliomagenesis a restrict number of neural stem cells and/or mature glial cells reaches a new steady state going from resting-cells homeostasis to the allostatic condition of cancer stem cells (CSCs). From our point of view the majority of the proteins present on CSCs plasma membrane is either upregulated or depressed in their quantity and/or function. In GBM cells ionic channels [46, 143] , transporters [144], proton pumps [145], membrane receptors [146] and also pro-oxidative mechanisms [132] have been previously described to be overexpressed, not present, hyper-activated or down regulated compared to control conditions. In this chronic allostatic system, a modification of any of these proteins produces a disruption of the new equilibrium and eventually results in the cell death. What is particularly problematic is that all the known proteins that are dysregulated in the tumorigenic process are also protein with important physiological roles in the homeostatic situation as well. Thus, if it is true that by hitting for example one of the overexpressed elements it may be possible to destroy the cancer stem cells, it is also realistic that healthy cells will be damaged by the same procedure. The idea, to design a successful therapy, is to identify proteins not only fundamental but also specific for the tumorigenic processes typical of CSCs. An unambiguous target will allow, once modulated, to impair only tumor cells avoiding serious collateral damages.

The experiments carried out in this thesis confirm that CLIC1 could be a valid candidate to match this specificity.

It has been shown that CLIC1 is functionally active and fundamental in the proliferation process of CSCs but not of MSCs (Figure 17). Moreover the channel activity inhibition obtained by the specific inhibitor IAA94 lead to accumulation of CSCs in G1 phase suggesting the need of CLIC1 mediated chloride current for the transition from G1 to S phase of the cell cycle (Figure 15).

Through immunolocalization of the protein and electrophysiological measurement of the chloride current we identified a precise timing in which CLIC1 accumulates at the membrane level. In CSCs CLIC1 activity reaches a maximum during the progression of G1 phase. When cells are synchronized in G1 and released, the current mediated by CLIC1 markedly increases and reaches a peak of amplitude around 8 hours later (Figure 21-22). At 18 hours from the release, when many of the cells are already progressed to S phase, the current significantly decreases and becomes comparable to the average current of randomly cycling cells (Figure 22). The fact that the randomly cycling cells show an average current density that is significantly lower compared to the current at 8 hours from the release suggests that the timing of the increase of the current is tightly regulated and that it happens in a very narrow time slot.

The literature proposes two principal factors regulating CLIC1 membrane insertion and channel activity: pH and ROS [4, 6, 7, 28, 45]. The thesis experimental work demonstrates that inducing CSCs cytoplasm alkalinization lead to an increase in the current mediated by CLIC1 (Figure 25-26). It is known that cancer cells display a high internal pH and there are some evidences for an oscillation of pH_i during cell cycle progression [95, 131]. We now found that in CSCs released from G1 arrest the pH_i peaks between 8 and 10 hours after the release reaching almost a value of 8 (Figure 23). This corresponds to the time in which CLIC1 chloride current results augmented.

The suggested regulation of CLIC1 activity by pH_i during cell cycle progression is confirmed by the inhibition of Na^+/H^+ exchanger 1 (NHE1). Releasing the cells in a medium containing EIPA, a specific NHE1 inhibitor, CLIC1 current increase is abolished both at 4 and 8 hours from the synchronization release (Figure 27). NHE1 is the exchanger responsible for most of the internal pH regulation in glioblastomas cells; an inhibition of NHE1 using EIPA will lead to acidification while an activation using FMLP will have the opposite effect (Figure 24). Thus, the increase in CLIC1 activity during the progression of G1 phase is related to an increased NHE1 activity.

The other factor known to regulate CLIC1 activity is the oxidative level of the cells. It has also been demonstrated that an increase in ROS level is fundamental for the progression from G1 to S phase of the cell cycle [55, 138] and that in glioblastoma cells the isoform 4 of NADPH oxidase (NOX) is overexpressed [132]. In addition, our data showed that ROS production is implicated also in the regulation of CLIC1 current observed during G1 progression. Indeed, when we release the cells after G1 synchronization in a medium containing the NOX inhibitor DPI, we were unable to record a significant increase of the current both at 4 and 8 hours from the release (Figure 30).

All the data we presented so far confirm CLIC1 involvement in the progression of the cell cycle and pave the way for uncovering the mechanism involved in the modulation of the channel activity. There are two important questions that are legitimate to ask:

a. Are the three elements equally influenced by the other two in case of a specific inhibitory action?

b. Considering only the three player during the progression of the cell cycle, is one of them responsible for the beginning of the process that moves the cells from the homeostatic to the allostatic conditions?

These questions are very important. Knowing the “on” mechanism it will be also possible to study the “off” process and in this way understanding the relations between the three components.

In a previous investigation involving the activation of microglia cells during infection of the central nervous system our laboratory described a positive feed-forward mechanism between ROS production and CLIC1 functional expression as an ion channel in the microglia cells membranes [45]

Activated microglia is an allostatic system in which all the three elements (CLIC1, NHE1 and NOX) are hyper-active and influence each other activity. When microglia is activated there is an increase in ROS levels. This increase is related to an augmented assembly on the membrane and a higher activity of NADPH oxidase [147]. From the literature about CLIC1 it is also known that this increased activity of NOX is associated with an increased activity of the channel [44, 45]. Moreover, as described in the introduction, it has been demonstrated that CLIC1 and NOX in activated microglia are part of a feed-forward mechanism. The NADPH oxidase by synthetizing ROS produces also an outward negative charge flow that need to be compensated. In this case it is required either a positive charge outflow or an inward movement of negative charges. Among all the possibilities represented mainly by potassium ions, CLIC1 has been identified in this contest to play a major role. In microglia cells activated by Aβ as an example, CLIC1 moves to the membrane where it forms an ion channel that mediates a chloride current necessary to support NOX activity [45]. Activated microglia and glioblastoma cells share also common mechanisms in the regulation of internal pH; NHE1 plays a key role in maintaining resting pH_i both in glioblastoma and in microglia cells [131, 139].

Moreover the activation of microglia is associated with an alkalinization of the cytoplasm due to an augmented NHE1 activity. This increased activity of NHE1 is stimulated by the increase in the activity of NOX since when the cells are treated with DPI the activation of the exchanger is reduced by 50% [139]. pH changes and ROS production have been proposed

to participate to a feed forward mechanism since the activity of NHE1 in the extrusion of H^+ produced by NADPH oxidase is fundamental to maintain the optimal pH_i necessary for the activity of the enzyme. When NHE1 is inhibited in activated microglia NOX activity is reduced [139].

All these similarities suggest for the presence of comparable mechanisms of mutual-support of the activities of CLIC1, NHE1 and NOX also in glioblastoma CSCs.

Our experiments prove that both the inhibition of CLIC1 current and NOX impair the pH_i regulation by NHE1. When NADPH oxidase is inhibited by DPI treatment both during an acute (30 minutes) and chronic (24 hours) treatment, pH_i decreases (Figure 31). Acidification is recovered if the DPI treatment is associated with an activation of NHE1 by FMLP confirming the regulation of NHE1 functioning by NOX (Figure 31). This is observed also in the regulation of CLIC1 current during cell cycle progression. The decrease of CLIC1 current at 8 hours from the release from G1 synchronization, that is observed when NADPH oxidase is inhibited, is partially recovered by the simultaneous activation of NHE1; these data suggest a double effect of NADPH oxidase on CLIC1 activity: one direct and one indirect through NHE1 (Figure 32).

The scenario of the effect of CLIC1 inhibitor IAA94 treatment on NHE1 is more complex. An acute treatment of 30 minutes leads to a hyper-activation of NHE1, recorded as an alkalinization that is counteracted by the co-treatment with the NHE1 inhibitor EIPA. On the other hand, a long treatment of 24 hours acidifies the cytosol of CSCs and the effect is not recovered by the treatment with FMLP (Figure 28). Moreover, the increase of pH_i observed during the progression of G1 phase seems to be limited when CLIC1 is inhibited by IAA94 treatment (Figure 29). We can speculate that this opposite effect could be due to an immediate compensative hyper-activation of NHE1 after CLIC1 inhibition that in the long run is progressively extinguished, since the channel activity is necessary to sustain the exchanger, leading to the opposite effect of acidification.

The first experiments to monitor the oxidative levels of the cells suggest an effect of IAA94 on ROS production (Figure 33). This could be interpreted as a CLIC1 current support of NADPH activity. These last experiments need to be confirmed and the effect of the short treatment with IAA94 need to be clarified. In the nearest future plan there is also the demonstration of an effect of NHE1 inhibition on the oxidative levels of CSCs as suggested from the literature and from all the other results obtained until now. This will in a way “close the circle” and shed light on the possibility that one of the three elements involved in this loop could be the trigger for its activation.

However, all the experiments presented in this thesis clearly confirm that in the allostatic system represented by CSCs there is a functional loop between the NHE1 exchanger, CLIC1 and the membrane NADPH oxidase, all of them overexpressed and upregulated in CSCs. During G1 phase progression the exchanger increases the cytoplasm pH, favoring CLIC1 channel activity. The increase in ROS levels through the activation of NADPH oxidase stimulates CLIC1 membrane insertion and sustains NHE1 activity. CLIC1 ionic current supports the work of both NADPH oxidase in the production of superoxide and NHE1 in the H^+ extrusion. In this scenario, all of these membrane proteins participate to the gliomagenesis sustaining CSCs cell cycle progression. To hamper this mechanism it is possible to act on each of the components. However, while NHE1 and NADPH oxidase are essential for brain cells homeostasis, CLIC1 chloride channels are present in the membrane exclusively in glioblastoma allostatic system making the channel protein the most attractive pharmacological target.

The parallel with the allostatic system of activated microglia, in which CLIC1, NHE1 and NADPH oxidase are all hyper-active and influence each other activity, besides sustaining our hypothesis, gives the possibility to study the interaction between the three elements in a system that is inducible. This could be of great help in defining the exact timing of the hyper-activation of every single factor and the influence of this activation on the activity of the others.

7. REFERENCES

References

1. Vescovi, A.L., R. Galli, and B.A. Reynolds, *Brain tumour stem cells.* Nat Rev Cancer, 2006. **6**(6): p. 425-36.
2. Reya, T., et al., *Stem cells, cancer, and cancer stem cells.* Nature, 2001. **414**(6859): p. 105-11.
3. Jones, T.S. and E.C. Holland, *Molecular pathogenesis of malignant glial tumors.* Toxicol Pathol, 2011. **39**(1): p. 158-66.
4. Tulk, B.M., S. Kapadia, and J.C. Edwards, *CLIC1 inserts from the aqueous phase into phospholipid membranes, where it functions as an anion channel.* Am J Physiol Cell Physiol, 2002. **282**(5): p. C1103-12.
5. Gritti, M., et al., *Metformin repositioning as antitumoral agent: selective antiproliferative effects in human glioblastoma stem cells, via inhibition of CLIC1-mediated ion current.* Oncotarget, 2014. **5**(22): p. 11252-68.
6. Goodchild, S.C., et al., *Oxidation promotes insertion of the CLIC1 chloride intracellular channel into the membrane.* Eur Biophys J, 2009. **39**(1): p. 129-38.
7. Littler, D.R., et al., *The intracellular chloride ion channel protein CLIC1 undergoes a redox-controlled structural transition.* J Biol Chem, 2004. **279**(10): p. 9298-305.
8. Kunzelmann, K., *Ion channels and cancer.* J Membr Biol, 2005. **205**(3): p. 159-73.
9. Prevarskaya, N., R. Skryma, and Y. Shuba, *Ion channels and the hallmarks of cancer.* Trends Mol Med, 2010. **16**(3): p. 107-21.
10. Pardo, L.A. and W. Stuhmer, *The roles of K(+) channels in cancer.* Nat Rev Cancer, 2014. **14**(1): p. 39-48.
11. Jentsch, T.J., et al., *Molecular structure and physiological function of chloride channels.* Physiol Rev, 2002. **82**(2): p. 503-68.
12. Succol, F., et al., *Intracellular chloride concentration influences the GABAA receptor subunit composition.* Nat Commun, 2012. **3**: p. 738.
13. Niisato, N., D.C. Eaton, and Y. Marunaka, *Involvement of cytosolic Cl- in osmoregulation of alpha-ENaC gene expression.* Am J Physiol Renal Physiol, 2004. **287**(5): p. F932-9.
14. Heimlich, G. and J.A. Cidlowski, *Selective role of intracellular chloride in the regulation of the intrinsic but not extrinsic pathway of apoptosis in Jurkat T-cells.* J Biol Chem, 2006. **281**(4): p. 2232-41.
15. Yang, T., et al., *Low chloride stimulation of prostaglandin E2 release and cyclooxygenase-2 expression in a mouse macula densa cell line.* J Biol Chem, 2000. **275**(48): p. 37922-9.
16. Voets, T., et al., *Blockers of volume-activated Cl- currents inhibit endothelial cell proliferation.* Pflugers Arch, 1995. **431**(1): p. 132-4.
17. Soroceanu, L., T.J. Manning, Jr., and H. Sontheimer, *Modulation of glioma cell migration and invasion using Cl(-) and K(+) ion channel blockers.* J Neurosci, 1999. **19**(14): p. 5942-54.
18. Schlichter, L.C., et al., *Properties of K+ and Cl- channels and their involvement in proliferation of rat microglial cells.* Glia, 1996. **17**(3): p. 225-36.
19. Gerard, V., et al., *Alterations of ionic membrane permeabilities in multidrug-resistant neuroblastoma x glioma hybrid cells.* J Exp Biol, 1998. **201**(Pt 1): p. 21-31.

20. Jiang, B., et al., *Expression and roles of Cl- channel ClC-5 in cell cycles of myeloid cells.* Biochem Biophys Res Commun, 2004. **317**(1): p. 192-7.
21. Bubien, J.K., et al., *Cell cycle dependence of chloride permeability in normal and cystic fibrosis lymphocytes.* Science, 1990. **248**(4961): p. 1416-9.
22. Ullrich, N. and H. Sontheimer, *Cell cycle-dependent expression of a glioma-specific chloride current: proposed link to cytoskeletal changes.* Am J Physiol, 1997. **273**(4 Pt 1): p. C1290-7.
23. Olsen, M.L., et al., *Expression of voltage-gated chloride channels in human glioma cells.* J Neurosci, 2003. **23**(13): p. 5572-82.
24. Lemonnier, L., et al., *Bcl-2-dependent modulation of swelling-activated Cl- current and ClC-3 expression in human prostate cancer epithelial cells.* Cancer Res, 2004. **64**(14): p. 4841-8.
25. Mao, J., et al., *Suppression of ClC-3 channel expression reduces migration of nasopharyngeal carcinoma cells.* Biochem Pharmacol, 2008. **75**(9): p. 1706-16.
26. Peretti, M., et al., *Chloride channels in cancer: Focus on chloride intracellular channel 1 and 4 (CLIC1 AND CLIC4) proteins in tumor development and as novel therapeutic targets.* Biochim Biophys Acta, 2014.
27. Landry, D., et al., *Molecular cloning and characterization of p64, a chloride channel protein from kidney microsomes.* J Biol Chem, 1993. **268**(20): p. 14948-55.
28. Averaimo, S., et al., *Chloride intracellular channel 1 (CLIC1): Sensor and effector during oxidative stress.* FEBS Lett, 2010. **584**(10): p. 2076-84.
29. Peter, B., et al., *Membrane mimetics induce helix formation and oligomerization of the chloride intracellular channel protein 1 transmembrane domain.* Biochemistry, 2013. **52**(16): p. 2739-49.
30. Valenzuela, S.M., et al., *Molecular cloning and expression of a chloride ion channel of cell nuclei.* J Biol Chem, 1997. **272**(19): p. 12575-82.
31. Howell, S., R.R. Duncan, and R.H. Ashley, *Identification and characterisation of a homologue of p64 in rat tissues.* FEBS Lett, 1996. **390**(2): p. 207-10.
32. Tonini, R., et al., *Functional characterization of the NCC27 nuclear protein in stable transfected CHO-K1 cells.* FASEB J, 2000. **14**(9): p. 1171-8.
33. Murzin, A.G., *Biochemistry. Metamorphic proteins.* Science, 2008. **320**(5884): p. 1725-6.
34. Singh, H., *Two decades with dimorphic Chloride Intracellular Channels (CLICs).* FEBS Lett, 2010. **584**(10): p. 2112-21.
35. Littler, D.R., et al., *The enigma of the CLIC proteins: Ion channels, redox proteins, enzymes, scaffolding proteins?* FEBS Lett, 2010. **584**(10): p. 2093-101.
36. Goodchild, S.C., et al., *Metamorphic response of the CLIC1 chloride intracellular ion channel protein upon membrane interaction.* Biochemistry, 2010. **49**(25): p. 5278-89.
37. Harrop, S.J., et al., *Crystal structure of a soluble form of the intracellular chloride ion channel CLIC1 (NCC27) at 1.4-A resolution.* J Biol Chem, 2001. **276**(48): p. 44993-5000.
38. Achilonu, I., et al., *Role of individual histidines in the pH-dependent global stability of human chloride intracellular channel 1.* Biochemistry, 2012. **51**(5): p. 995-1004.
39. Valenzuela, S.M., et al., *The nuclear chloride ion channel NCC27 is involved in regulation of the cell cycle.* J Physiol, 2000. **529 Pt 3**: p. 541-52.
40. Behrend, L., G. Henderson, and R.M. Zwacka, *Reactive oxygen species in oncogenic transformation.* Biochem Soc Trans, 2003. **31**(Pt 6): p. 1441-4.
41. Boillee, S. and D.W. Cleveland, *Revisiting oxidative damage in ALS: microglia, Nox, and mutant SOD1.* J Clin Invest, 2008. **118**(2): p. 474-8.

42. Thomas, M.P., et al., *Ion channel blockade attenuates aggregated alpha synuclein induction of microglial reactive oxygen species: relevance for the pathogenesis of Parkinson's disease.* J Neurochem, 2007. **100**(2): p. 503-19.
43. Perry, G., A.D. Cash, and M.A. Smith, *Alzheimer Disease and Oxidative Stress.* J Biomed Biotechnol, 2002. **2**(3): p. 120-123.
44. Novarino, G., et al., *Involvement of the intracellular ion channel CLIC1 in microglia-mediated beta-amyloid-induced neurotoxicity.* J Neurosci, 2004. **24**(23): p. 5322-30.
45. Milton, R.H., et al., *CLIC1 function is required for beta-amyloid-induced generation of reactive oxygen species by microglia.* J Neurosci, 2008. **28**(45): p. 11488-99.
46. Setti, M., et al., *Functional role of CLIC1 ion channel in glioblastoma-derived stem/progenitor cells.* J Natl Cancer Inst, 2013. **105**(21): p. 1644-55.
47. Wulfkuhle, J.D., et al., *Proteomics of human breast ductal carcinoma in situ.* Cancer Res, 2002. **62**(22): p. 6740-9.
48. Chen, C.D., et al., *Overexpression of CLIC1 in human gastric carcinoma and its clinicopathological significance.* Proteomics, 2007. **7**(1): p. 155-67.
49. Wang, J.W., et al., *Identification of metastasis-associated proteins involved in gallbladder carcinoma metastasis by proteomic analysis and functional exploration of chloride intracellular channel 1.* Cancer Lett, 2009. **281**(1): p. 71-81.
50. Petrova, D.T., et al., *Expression of chloride intracellular channel protein 1 (CLIC1) and tumor protein D52 (TPD52) as potential biomarkers for colorectal cancer.* Clin Biochem, 2008. **41**(14-15): p. 1224-36.
51. Chang, Y.H., et al., *Cell secretome analysis using hollow fiber culture system leads to the discovery of CLIC1 protein as a novel plasma marker for nasopharyngeal carcinoma.* J Proteome Res, 2009. **8**(12): p. 5465-74.
52. Tang, H.Y., et al., *A xenograft mouse model coupled with in-depth plasma proteome analysis facilitates identification of novel serum biomarkers for human ovarian cancer.* J Proteome Res, 2012. **11**(2): p. 678-91.
53. Zhang, J., et al., *Clic1 plays a role in mouse hepatocarcinoma via modulating Annexin A7 and Gelsolin in vitro and in vivo.* Biomed Pharmacother, 2015. **69**: p. 416-9.
54. Wang, L., et al., *Elevated expression of chloride intracellular channel 1 is correlated with poor prognosis in human gliomas.* J Exp Clin Cancer Res, 2012. **31**: p. 44.
55. Menon, S.G. and P.C. Goswami, *A redox cycle within the cell cycle: ring in the old with the new.* Oncogene, 2007. **26**(8): p. 1101-9.
56. Stupp, R., et al., *High-grade malignant glioma: ESMO Clinical Practice Guidelines for diagnosis, treatment and follow-up.* Annals of Oncology, 2010. **21**: p. v190-v193.
57. Schwartzbaum, J.A., et al., *Epidemiology and molecular pathology of glioma.* Nat Clin Pract Neurol, 2006. **2**(9): p. 494-503; quiz 1 p following 516.
58. Sanai, N., A. Alvarez-Buylla, and M.S. Berger, *Neural stem cells and the origin of gliomas.* N Engl J Med, 2005. **353**(8): p. 811-22.
59. Louis, D.N., et al., *The 2007 WHO classification of tumours of the central nervous system.* Acta Neuropathologica, 2007. **114**(2): p. 97-109.
60. Behin, A., et al., *Primary brain tumours in adults.* Lancet, 2003. **361**(9354): p. 323-31.
61. Wen, P.Y. and S. Kesari, *Malignant gliomas in adults.* N Engl J Med, 2008. **359**(5): p. 492-507.
62. Kleihues, P. and H. Ohgaki, *Primary and secondary glioblastomas: from concept to clinical diagnosis.* Neuro Oncol, 1999. **1**(1): p. 44-51.
63. Maher, E.A., et al., *Malignant glioma: genetics and biology of a grave matter.* Genes Dev, 2001. **15**(11): p. 1311-33.

64. Hill, C., S.B. Hunter, and D.J. Brat, *Genetic markers in glioblastoma: prognostic significance and future therapeutic implications.* Adv Anat Pathol, 2003. **10**(4): p. 212-7.
65. Singh, S.K., et al., *Identification of human brain tumour initiating cells.* Nature, 2004. **432**(7015): p. 396-401.
66. Fomchenko, E.I. and E.C. Holland, *Stem cells and brain cancer.* Exp Cell Res, 2005. **306**(2): p. 323-9.
67. Potten, C.S. and M. Loeffler, *Stem cells: attributes, cycles, spirals, pitfalls and uncertainties. Lessons for and from the crypt.* Development, 1990. **110**(4): p. 1001-20.
68. Bonnet, D. and J.E. Dick, *Human acute myeloid leukemia is organized as a hierarchy that originates from a primitive hematopoietic cell.* Nat Med, 1997. **3**(7): p. 730-7.
69. Ignatova, T.N., et al., *Human cortical glial tumors contain neural stem-like cells expressing astroglial and neuronal markers in vitro.* Glia, 2002. **39**(3): p. 193-206.
70. Hemmati, H.D., et al., *Cancerous stem cells can arise from pediatric brain tumors.* Proc Natl Acad Sci U S A, 2003. **100**(25): p. 15178-83.
71. Galli, R., et al., *Isolation and characterization of tumorigenic, stem-like neural precursors from human glioblastoma.* Cancer Res, 2004. **64**(19): p. 7011-21.
72. Chen, J., et al., *A restricted cell population propagates glioblastoma growth after chemotherapy.* Nature, 2012. **488**(7412): p. 522-6.
73. Bao, S., et al., *Glioma stem cells promote radioresistance by preferential activation of the DNA damage response.* Nature, 2006. **444**(7120): p. 756-60.
74. Denysenko, T., et al., *Glioblastoma cancer stem cells: heterogeneity, microenvironment and related therapeutic strategies.* Cell Biochem Funct, 2010. **28**(5): p. 343-51.
75. Binda, E., B.A. Reynolds, and A.L. Vescovi, *Glioma stem cells: turpis omen in nomen? (The evil in the name?).* J Intern Med, 2014. **276**(1): p. 25-40.
76. Lathia, J.D., et al., *Cancer stem cells in glioblastoma.* Genes Dev, 2015. **29**(12): p. 1203-17.
77. Visvader, J.E. and G.J. Lindeman, *Cancer stem cells in solid tumours: accumulating evidence and unresolved questions.* Nat Rev Cancer, 2008. **8**(10): p. 755-68.
78. Dirks, P.B., *Brain tumor stem cells: bringing order to the chaos of brain cancer.* J Clin Oncol, 2008. **26**(17): p. 2916-24.
79. Dirks, P.B., *Brain tumor stem cells: the cancer stem cell hypothesis writ large.* Mol Oncol, 2010. **4**(5): p. 420-30.
80. Ben-Porath, I., et al., *An embryonic stem cell-like gene expression signature in poorly differentiated aggressive human tumors.* Nat Genet, 2008. **40**(5): p. 499-507.
81. Ligon, K.L., et al., *Olig2-regulated lineage-restricted pathway controls replication competence in neural stem cells and malignant glioma.* Neuron, 2007. **53**(4): p. 503-17.
82. Kim, J., et al., *A Myc network accounts for similarities between embryonic stem and cancer cell transcription programs.* Cell, 2010. **143**(2): p. 313-24.
83. Tunici, P., et al., *Genetic alterations and in vivo tumorigenicity of neurospheres derived from an adult glioblastoma.* Mol Cancer, 2004. **3**: p. 25.
84. Anido, J., et al., *TGF-beta Receptor Inhibitors Target the CD44(high)/Id1(high) Glioma-Initiating Cell Population in Human Glioblastoma.* Cancer Cell, 2010. **18**(6): p. 655-68.
85. Son, M.J., et al., *SSEA-1 is an enrichment marker for tumor-initiating cells in human glioblastoma.* Cell Stem Cell, 2009. **4**(5): p. 440-52.

86. Liu, G., et al., *Analysis of gene expression and chemoresistance of CD133+ cancer stem cells in glioblastoma.* Mol Cancer, 2006. **5**: p. 67.
87. Bao, S., et al., *Targeting cancer stem cells through L1CAM suppresses glioma growth.* Cancer Res, 2008. **68**(15): p. 6043-8.
88. Ogden, A.T., et al., *Identification of A2B5+CD133- tumor-initiating cells in adult human gliomas.* Neurosurgery, 2008. **62**(2): p. 505-14; discussion 514-5.
89. Lathia, J.D., et al., *Integrin alpha 6 regulates glioblastoma stem cells.* Cell Stem Cell, 2010. **6**(5): p. 421-32.
90. Bhat, K.P., et al., *Mesenchymal differentiation mediated by NF-kappaB promotes radiation resistance in glioblastoma.* Cancer Cell, 2013. **24**(3): p. 331-46.
91. Bleau, A.M. and E.C. Holland, *[Chemotherapeutic treatment of gliomas increases the amount of cancer stem-like cells].* Med Sci (Paris), 2009. **25**(10): p. 775-7.
92. Golebiewska, A., et al., *Side population in human glioblastoma is non-tumorigenic and characterizes brain endothelial cells.* Brain, 2013. **136**(Pt 5): p. 1462-75.
93. Broadley, K.W., et al., *Side population is not necessary or sufficient for a cancer stem cell phenotype in glioblastoma multiforme.* Stem Cells, 2011. **29**(3): p. 452-61.
94. Fidelman, M.L., et al., *Intracellular pH mediates action of insulin on glycolysis in frog skeletal muscle.* Am J Physiol, 1982. **242**(1): p. C87-93.
95. Madshus, I.H., *Regulation of intracellular pH in eukaryotic cells.* Biochem J, 1988. **250**(1): p. 1-8.
96. Pouyssegur, J., et al., *Cytoplasmic pH, a key determinant of growth factor-induced DNA synthesis in quiescent fibroblasts.* FEBS Lett, 1985. **190**(1): p. 115-9.
97. Mills, G.B., et al., *Interleukin 2 induces a rapid increase in intracellular pH through activation of a Na+/H+ antiport. Cytoplasmic alkalinization is not required for lymphocyte proliferation.* J Biol Chem, 1985. **260**(23): p. 12500-7.
98. Lagana, A., et al., *Regulation of the formation of tumor cell pseudopodia by the Na(+)/H(+) exchanger NHE1.* J Cell Sci, 2000. **113 (Pt 20)**: p. 3649-62.
99. Harguindey, S., et al., *The role of pH dynamics and the Na+/H+ antiporter in the etiopathogenesis and treatment of cancer. Two faces of the same coin--one single nature.* Biochim Biophys Acta, 2005. **1756**(1): p. 1-24.
100. Murer, H., U. Hopfer, and R. Kinne, *Sodium/proton antiport in brush-border-membrane vesicles isolated from rat small intestine and kidney.* Biochem J, 1976. **154**(3): p. 597-604.
101. Simchowitz, L., *Intracellular pH modulates the generation of superoxide radicals by human neutrophils.* J Clin Invest, 1985. **76**(3): p. 1079-89.
102. Moolenaar, W.H., et al., *Epidermal growth factor induces electrically silent Na+ influx in human fibroblasts.* J Biol Chem, 1982. **257**(14): p. 8502-6.
103. Reshkin, S.J., M.R. Greco, and R.A. Cardone, *Role of pHi, and proton transporters in oncogene-driven neoplastic transformation.* Philos Trans R Soc Lond B Biol Sci, 2014. **369**(1638): p. 20130100.
104. Burdon, R.H., V. Gill, and C. Rice-Evans, *Cell proliferation and oxidative stress.* Free Radic Res Commun, 1989. **7**(3-6): p. 149-59.
105. Burdon, R.H. and C. Rice-Evans, *Free radicals and the regulation of mammalian cell proliferation.* Free Radic Res Commun, 1989. **6**(6): p. 345-58.
106. Suzuki, Y.J., H.J. Forman, and A. Sevanian, *Oxidants as stimulators of signal transduction.* Free Radic Biol Med, 1997. **22**(1-2): p. 269-85.
107. Halliwell, B., *Free radicals, proteins and DNA: oxidative damage versus redox regulation.* Biochem Soc Trans, 1996. **24**(4): p. 1023-7.

108. Halliwell, B. and J.M. Gutteridge, *Biologically relevant metal ion-dependent hydroxyl radical generation. An update.* FEBS Lett, 1992. **307**(1): p. 108-12.
109. Massey, V., et al., *The production of superoxide anion radicals in the reaction of reduced flavins and flavoproteins with molecular oxygen.* Biochem Biophys Res Commun, 1969. **36**(6): p. 891-7.
110. Bokoch, G.M. and U.G. Knaus, *NADPH oxidases: not just for leukocytes anymore!* Trends Biochem Sci, 2003. **28**(9): p. 502-8.
111. Schrader, M. and H.D. Fahimi, *Mammalian peroxisomes and reactive oxygen species.* Histochem Cell Biol, 2004. **122**(4): p. 383-93.
112. Zangar, R.C., D.R. Davydov, and S. Verma, *Mechanisms that regulate production of reactive oxygen species by cytochrome P450.* Toxicol Appl Pharmacol, 2004. **199**(3): p. 316-31.
113. Klebanoff, S.J., *Myeloperoxidase: friend and foe.* J Leukoc Biol, 2005. **77**(5): p. 598-625.
114. Veal, E.A., et al., *A 2-Cys peroxiredoxin regulates peroxide-induced oxidation and activation of a stress-activated MAP kinase.* Mol Cell, 2004. **15**(1): p. 129-39.
115. Wood, Z.A., L.B. Poole, and P.A. Karplus, *Peroxiredoxin evolution and the regulation of hydrogen peroxide signaling.* Science, 2003. **300**(5619): p. 650-3.
116. Zhao, R. and A. Holmgren, *A novel antioxidant mechanism of ebselen involving ebselen diselenide, a substrate of mammalian thioredoxin and thioredoxin reductase.* J Biol Chem, 2002. **277**(42): p. 39456-62.
117. Di Mascio, P., M.E. Murphy, and H. Sies, *Antioxidant defense systems: the role of carotenoids, tocopherols, and thiols.* Am J Clin Nutr, 1991. **53**(1 Suppl): p. 194S-200S.
118. Suzuki, R.M.D.Y.J., *Cell Proliferation, Reactive Oxygen and Cellular Glutathione.* Dose Response, 2005. **3**(3): p. 425-442.
119. L., R., *Su les processus chimiques au cours de la division cellulaire.* Ann Physiol Physiochem Biol, 1931. **7**: p. 382-418.
120. Mauro, F., A. Grasso, and L.J. Tolmach, *Variations in sulfhydryl, disulfide, and protein content during synchronous and asynchronous growth of HeLa cells.* Biophys J, 1969. **9**(11): p. 1377-97.
121. Tu, B.P., et al., *Logic of the yeast metabolic cycle: temporal compartmentalization of cellular processes.* Science, 2005. **310**(5751): p. 1152-8.
122. Burdon, R.H. and V. Gill, *Cellularly generated active oxygen species and HeLa cell proliferation.* Free Radic Res Commun, 1993. **19**(3): p. 203-13.
123. Conour, J.E., W.V. Graham, and H.R. Gaskins, *A combined in vitro/bioinformatic investigation of redox regulatory mechanisms governing cell cycle progression.* Physiol Genomics, 2004. **18**(2): p. 196-205.
124. Oberley, T.D., et al., *Antioxidant enzyme levels as a function of growth state in cell culture.* Free Radic Biol Med, 1995. **19**(1): p. 53-65.
125. Sarsour, E.H., et al., *Redox control of the cell cycle in health and disease.* Antioxid Redox Signal, 2009. **11**(12): p. 2985-3011.
126. Menon, S.G., et al., *Differential susceptibility of nonmalignant human breast epithelial cells and breast cancer cells to thiol antioxidant-induced G(1)-delay.* Antioxid Redox Signal, 2005. **7**(5-6): p. 711-8.
127. Oberley, L.W., T.D. Oberley, and G.R. Buettner, *Cell division in normal and transformed cells: the possible role of superoxide and hydrogen peroxide.* Med Hypotheses, 1981. **7**(1): p. 21-42.

128. Burhans, W.C. and N.H. Heintz, *The cell cycle is a redox cycle: linking phase-specific targets to cell fate.* Free Radic Biol Med, 2009. **47**(9): p. 1282-93.
129. Hubesch, B., et al., *P-31 MR spectroscopy of normal human brain and brain tumors.* Radiology, 1990. **174**(2): p. 401-9.
130. Shrode, L.D. and R.W. Putnam, *Intracellular pH regulation in primary rat astrocytes and C6 glioma cells.* Glia, 1994. **12**(3): p. 196-210.
131. McLean, L.A., et al., *Malignant gliomas display altered pH regulation by NHE1 compared with nontransformed astrocytes.* Am J Physiol Cell Physiol, 2000. **278**(4): p. C676-88.
132. Shono, T., et al., *Enhanced expression of NADPH oxidase Nox4 in human gliomas and its roles in cell proliferation and survival.* Int J Cancer, 2008. **123**(4): p. 787-92.
133. Hsieh, C.H., et al., *NADPH oxidase subunit 4-mediated reactive oxygen species contribute to cycling hypoxia-promoted tumor progression in glioblastoma multiforme.* PLoS One, 2011. **6**(9): p. e23945.
134. Hsieh, C.H., et al., *NADPH oxidase subunit 4 mediates cycling hypoxia-promoted radiation resistance in glioblastoma multiforme.* Free Radic Biol Med, 2012. **53**(4): p. 649-58.
135. Hamill, O.P., et al., *Improved patch-clamp techniques for high-resolution current recording from cells and cell-free membrane patches.* Pflugers Arch, 1981. **391**(2): p. 85-100.
136. Chow, S. and D. Hedley, *Flow cytometric measurement of intracellular pH.* Curr Protoc Cytom, 2001. **Chapter 9**: p. Unit 9 3.
137. Waypa, G.B., et al., *Hypoxia triggers subcellular compartmental redox signaling in vascular smooth muscle cells.* Circ Res, 2010. **106**(3): p. 526-35.
138. Menon, S.G., et al., *Redox regulation of the G1 to S phase transition in the mouse embryo fibroblast cell cycle.* Cancer Res, 2003. **63**(9): p. 2109-17.
139. Liu, Y., et al., *Activation of microglia depends on Na+/H+ exchange-mediated H+ homeostasis.* J Neurosci, 2010. **30**(45): p. 15210-20.
140. Morgan, D., et al., *The pH dependence of NADPH oxidase in human eosinophils.* J Physiol, 2005. **569**(Pt 2): p. 419-31.
141. McEwen, B.S., *Stress, adaptation, and disease. Allostasis and allostatic load.* Ann N Y Acad Sci, 1998. **840**: p. 33-44.
142. McEwen, B.S. and J.C. Wingfield, *The concept of allostasis in biology and biomedicine.* Horm Behav, 2003. **43**(1): p. 2-15.
143. Molenaar, R.J., *Ion channels in glioblastoma.* ISRN Neurol, 2011. **2011**: p. 590249.
144. Cuddapah, V.A. and H. Sontheimer, *Ion channels and transporters [corrected] in cancer. 2. Ion channels and the control of cancer cell migration.* Am J Physiol Cell Physiol, 2011. **301**(3): p. C541-9.
145. Chesler, M., *Regulation and modulation of pH in the brain.* Physiol Rev, 2003. **83**(4): p. 1183-221.
146. Schlenska-Lange, A., et al., *Cell proliferation and migration in glioblastoma multiforme cell lines are influenced by insulin-like growth factor I in vitro.* Anticancer Res, 2008. **28**(2A): p. 1055-60.
147. Bianca, V.D., et al., *beta-amyloid activates the O-2 forming NADPH oxidase in microglia, monocytes, and neutrophils. A possible inflammatory mechanism of neuronal damage in Alzheimer's disease.* J Biol Chem, 1999. **274**(22): p. 15493-9.